A NOVEL APPROACH TO THE DYNAMICS OF FLEXIBLE BEAMS UNDER OVERALL MOTIONS – THE PLANE CASE

by

J. C. Simo and L. Vu Quoc

Memorandum No. UCB/ERL M85/63

31 August 1985

A NOVEL APPROACH TO THE DYNAMICS OF FLEXIBLE BEAMS UNDER LARGE OVERALL MOTIONS - THE PLANE CASE

by

J. C. Simo and L. Vu Quoc

Memorandum No. UCB/ERL M85/63

31 August 1985

ELECTRONICS RESEARCH LABORATORY

College of Engineering
University of California, Berkeley
94720

A Novel Approach to the Dynamics of Flexible Beams under large overall motions — The plane case.

J.C. SIMO

Applied Mechanics Division, Stanford University, Stanford, CA 94305.

and

L. VU QUOC

Structural Engineering and Structural Mechanics Division,
University of California, Berkeley, CA 94720.

Abstract

Traditionally, the dynamics of a flexible beam subject to large overall motions Is formulated relative to a floating frame, often referred to as *shadow beam*. This type of formulation leads to a set of equations of motion that are nonlinear and highly coupled in the inertia terms, of the form $\tilde{\mathbf{g}}(\dot{\mathbf{y}}, \mathbf{y}, t) = 0$. By contrast, we propose an alternative approach in which all quantities are referred to the *inertial* frame. As a result, the inertia term enters linearly in the formulation simply as mass times acceleration. Crucial to this formulation is the use of finite strain rod theories capable of undergoing finite rotations. Upon discretizing the spatial variables, the semi-discrete equations of motion have the standard explicit form: $\mathbf{M}\ddot{\mathbf{q}} + \mathbf{P}(\mathbf{q}) = \mathbf{F}$. Numerical examples that involve finite vibrations coupled with large overall motions are presented. These simulations also demonstrate the capability of the present formulation in handling *multibody dynamics*.

Contents

August 1, 1985

Introduction

The dynamics of a flexible beam undergoing large overall motions, is typically formulated relative to a coordinate system that follows the rigid body motion of the beam and is often referred to as *shadow beam* (Laskin, Likins & Longman [1983]). The introduction of this floating frame, relative to which the strains in the beam are measured, is motivated by the assumption of infinitesimal strains (see, e.g., Ashley [1967], Grote, McMunn & Gluck [1971], de Veubeke [1976], Canavin & Likins [1977], Kumar & Bainum [1980], Kane & Levinson [1981], Kane, Likins & Levinson [1983]). With the assumption of small strains, the use of floating frame allows a simple expression for the total potential energy of the beam. By contrast, the kinetic energy of the system takes a rather cumbersome form. The resulting equations of motion, although restricted to small strains, are *nonlinear* and *highly coupled* in the inertia terms due to the presence of Coriolis and centrifugal effects as well as inertia due to rotation of the shadow beam. Moreover, the Galerkin discretization in space variables, leads to a system of *implicit* coupled *nonlinear* differential equations in time of the form $\tilde{\mathbf{g}}(\dot{\mathbf{y}}, \mathbf{y}, t) = 0$ (e.g., Song & Haug [1980]). An essential characteristic of this system is that it cannot be transformed to a standard explicit form $\dot{\mathbf{y}} = \mathbf{g}(\mathbf{y}, t)$. Thus, use of the mode shapes of the structure as Galerkin basis, a procedure often employed (see, e.g., Likins [1974a]) appears to be of little value in the general case due to the highly coupled nature of the resulting semi-discrete equations. Moreover, the complex nature of these equations has often led to simplifying assumptions, e.g., Winfrey [1971], Erdman & Sandor [1972], Baghat & Willmert [1973]; we refer to Song & Haug [1980] for a review of several approaches in the dynamic analysis of mechanisms and machines.

In this paper, we propose an approach based on a philosophy opposite to that outlined above. The kinetic energy of the system is reduced to a quadratic uncoupled form simply by referring the motion of the system to the *inertial frame*. This results in a drastic simplification of the inertia operator, which now becomes *linear* and *uncoupled*, while the stiffness operator emanating from the potential energy functional becomes nonlinear. Conceptually, the essential step needed in developing this alternative approach is the use of rod theories capable of accounting for large rotations in the beam. It is important to note that the basic characteristic of the appropriate strain measures in these theories is their *invariance under superposed rigid body motions*; see Reissner [1972], Antman [1972,1974], Simo [1985], and Simo & Vu Quoc [1985].

From a computational standpoint, the substantial advantage of the proposed approach over the traditional shadow beam approach lies in a much simpler structure of the resulting equations. By introducing a Galerkin semi-discretization of these equations in the space variables, one obtains the standard nonlinear system of ODE's that typically arises in nonlinear structural dynamics: $\mathbf{M}\ddot{\mathbf{q}} + \mathbf{P}(\mathbf{q}) = \mathbf{F}$ (see, e.g., Belytschko & Hughes [1983]). In addition, this approach has the advantage of automatically accounting for large strains. Within the present context, there is little to be gained by introducing at the outset the additional small strains assumption.

As a basis of our discussion, we choose a specific problem to introduce our formulation: the dynamics of a flexible robot arm. This model problem consists of a flexible beam with one end at the origin of the inertial frame $\{\mathbf{e}_1, \mathbf{e}_2, \mathbf{e}_3\}$ (see Fig. 2.1). The robot arm is allowed to rotate about the axis $\mathbf{e}_3$, but the entire motions of the arm are restrained to the plane $\{\mathbf{e}_1, \mathbf{e}_2\}$. It will become clear, however, that our formulation can be applied to a more general setting of flexible plane beams subject to large overall motions. We shall also show through numerical examples that our formulation can be employed directly in the

analysis of a system of flexible beams connected by hinges, i.e., the *multibody dynamics* problem.

2. Classical approach based on small strains: Floating frame.

In this section we summarize the equations of motion for a rotating flexible beam under the assumption of small strains superposed onto large rigid body rotations using the shadow beam approach. The introduction of this floating frame, relative to which the strains in the beam are measured, is motivated by the assumption of infinitesimal strains. The essential purpose of the discussion that follows is to exhibit the main drawback of this approach. The introduction of the floating frame, although allowing a simple expression for the potential energy due to the assumption of infinitesimal strains, leads to a cumbersome expression for the kinetic energy of the system. This results in equations of motion with highly coupled nonlinear terms involving the time derivatives of the state variables. From a computational standpoint, the numerical integration of these equations is a nontrivial task.

2.1. Basic kinematic assumption

Consider the rotating bean shown in Fig. 2.1. Let $\boldsymbol{\phi}$ be the position vector of a material particle initially located at $\mathbf{X} = X_1\,\mathbf{e}_1 + X_2\,\mathbf{e}_2$ in the *undeformed* (reference) configuration. Here $\{\mathbf{e}_1, \mathbf{e}_2\}$ is the inertial frame attached to the fixed undeformed configuration. In addition, we introduce a floating frame $\{\mathbf{a}_1(t), \mathbf{a}_2(t)\}$ that follows the rigid body motion of the beam; i.e., the shadow beam. The basic kinematic assumption is expressed as

$$\boldsymbol{\phi}(X_1, X_2, t) := \tilde{\boldsymbol{\phi}}_0(X_1, t) + X_2\,\mathbf{t}_2(X_1, t) \tag{2.1a}$$

where

$$\begin{aligned} \tilde{\boldsymbol{\phi}}_0(X_1, t) &:= [X_1 + \tilde{u}_1(X_1, t)]\,\mathbf{a}_1(t) + \tilde{u}_2(X_1, t)\,\mathbf{a}_2(t) \\ \mathbf{t}_1(X_1, t) &:= \cos\tilde{\alpha}(X_1, t)\,\mathbf{a}_1(t) + \sin\tilde{\alpha}(X_1, t)\,\mathbf{a}_2(t) \\ \mathbf{t}_2(X_1, t) &:= -\sin\tilde{\alpha}(X_1, t)\,\mathbf{a}_1(t) + \cos\tilde{\alpha}(X_1, t)\,\mathbf{a}_2(t) \end{aligned} \tag{2.1b}$$

For notational simplicity, explicit indication of the arguments X_1, X_2 and t will often be omitted. Since the motion is planar, one has $\mathbf{e}_3 \equiv \mathbf{t}_3 \equiv \mathbf{a}_3$. Note that $\{\mathbf{t}_1, \mathbf{t}_2\}$ defines a moving frame that follows the deformation of the beam with $\mathbf{t}_2$ always contained in the deformed cross section and $\mathbf{t}_1$ perpendicular to the cross section. Using matrix notation, relations $(2.1b)_{2,3}$ may be expressed as

$$\begin{Bmatrix} \mathbf{t}_1 \\ \mathbf{t}_2 \end{Bmatrix} = \tilde{\boldsymbol{\Lambda}}^t \begin{Bmatrix} \mathbf{a}_1 \\ \mathbf{a}_2 \end{Bmatrix}, \quad \text{where} \quad \tilde{\boldsymbol{\Lambda}} := \begin{bmatrix} \cos\tilde{\alpha} & -\sin\tilde{\alpha} \\ \sin\tilde{\alpha} & \cos\tilde{\alpha} \end{bmatrix} \tag{2.2}$$

Although it is possible to develop the formulation without introducing any restriction on the size of the strain field, the assumption of small strains is typically introduced *ab-initio*, as discussed below.

2.2. Motivation: Total potential energy.

The introduction of the floating frame $\{\mathbf{a}_1, \mathbf{a}_2\}$ allows the enforcement at the outset of the following *infinitesimal strains* assumption.

$$\begin{aligned} &\tilde{\alpha} \quad \textbf{small} \quad (\leq 10^\circ) \iff \tilde{\boldsymbol{\Lambda}} \cong \begin{bmatrix} 1 & -\tilde{\alpha} \\ \tilde{\alpha} & 1 \end{bmatrix} \\ &\tilde{u}_1, \quad \text{and} \quad \tilde{u}_2 \quad \textbf{small} \end{aligned} \tag{2.3}$$

With this assumption in force, the strains $\tilde{\gamma}$ and curvature $\tilde{\kappa}$ relative to the floating frame $\{\mathbf{a}_1, \mathbf{a}_2\}$ are defined as

$$\tilde{\gamma} = \tilde{\phi}'_0 - \mathbf{t}_1, \qquad \kappa = \tilde{\alpha}' \mathbf{t}_3, \tag{2.4a}$$

where $(\cdot)' := d(\cdot)/dX_1$. In component form, $\tilde{\gamma}$ is expressed as

$$\tilde{\gamma} = \tilde{\gamma}_1 \mathbf{a}_1 + \tilde{\gamma}_2 \mathbf{a}_2 \tag{2.4b}$$

where

$$\tilde{\gamma}_1 = \tilde{u}'_1, \quad \tilde{\gamma}_2 = \tilde{u}'_2 - \tilde{\alpha} \tag{2.4c}$$

One refers to $\tilde{\gamma}_1$ and $\tilde{\gamma}_2$ as the *axial* strain and the *shearing* strain, respectively. Denoting by EA, GA_s and EI the axial, shear and flexural stiffnesses of the beam (relative to the floating frame $\{\mathbf{a}_1, \mathbf{a}_2\}$), the potential energy of the beam may be expressed as

$$\Pi := \tfrac{1}{2} \int_{[0,L]} \{EA\tilde{\gamma}_1^2 + GA_s\tilde{\gamma}_2^2 + EI\tilde{\alpha}'^2\}\, dS + \Pi_{EXT} - T(t)\psi(t) \tag{2.5}$$

where Π_{EXT} is the potential energy of the external loading acting on the beam and $T(t)\mathbf{e}_3$ is the applied torque at the axis of rotation $\mathbf{e}_3$ of the robot arm. Next, we proceed to compute the kinetic energy of the system.

2.3. Kinetic energy

By contrast with the simplicity of (2.5), the kinetic energy of the system takes a rather cumbersome form. To obtain the appropriate expression, we introduce the time derivative *relative to an observer attached to the floating frame*, defined as

$$\overset{\nabla}{\phi} := \left.\frac{\partial \phi}{\partial t}\right|_{\mathbf{a}_I = fixed} \tag{2.6}$$

We then have the following standard expression from rigid body mechanics (e.g. Goldstein [1980])

$$\dot{\phi} = \overset{\nabla}{\phi} + \mathbf{w} \times \phi \tag{2.7}$$

where, a superposed "dot" denotes material time derivative, and $\mathbf{w}$ is the angular velocity of the floating frame. For the plane under consideration, the angular velocity $\mathbf{w}$ is given simply as

$$\mathbf{w} = \frac{d\psi}{dt}\mathbf{a}_3 \equiv \dot{\psi}\mathbf{a}_3 \tag{2.8}$$

where $\mathbf{a}_3 := \mathbf{a}_1 \times \mathbf{a}_2$ is *fixed*. Upon noting that the the time derivative of the floating basis is given by

$$\dot{\mathbf{a}}_1 = \dot{\psi}\mathbf{a}_2, \qquad \dot{\mathbf{a}}_2 = -\dot{\psi}\mathbf{a}_1, \tag{2.9}$$

It follows from at once from expressions (2.1b) that the time derivative of the vectors $\{\mathbf{t}_1, \mathbf{t}_2\}$ is given by

$$\dot{\mathbf{t}}_1 = (\dot{\tilde{\alpha}} + \dot{\psi})\mathbf{t}_2, \qquad \dot{\mathbf{t}}_2 = -(\dot{\tilde{\alpha}} + \dot{\psi})\mathbf{t}_1 \tag{2.10}$$

Thus, the time derivative of the position vector ϕ is given by the following expression

$$\dot{\phi} = \overset{\nabla}{\phi}_0 + \dot{\psi}[-\tilde{u}_2\mathbf{a}_1 + (X_1 + \tilde{u}_1)\mathbf{a}_2] - X_2(\dot{\tilde{\alpha}} + \dot{\psi})\mathbf{t}_1 \tag{2.11a}$$

$$\overset{\nabla}{\phi}_0 = \dot{\tilde{u}}_1\mathbf{a}_1 + \dot{\tilde{u}}_2\mathbf{a}_2 \tag{2.11b}$$

The kinetic energy of the system is given by the expression

$$K := \int_{[0,L]\times[-\frac{h}{2},\frac{h}{2}]} \rho(X_1,X_2)\,\|\dot{\boldsymbol{\phi}}\|^2\,dX_1\,dX_2 \tag{2.12}$$

where $\rho(X_1,X_2)$ is the density and $\|\dot{\boldsymbol{\phi}}\|^2 := \dot{\varphi}_1^2 + \dot{\varphi}_2^2$. By substituting (2.11) into (2.12) we arrive at the following expression for the kinetic energy

$$\boxed{\begin{aligned} K = \; & \tfrac{1}{2}\int_{[0,L]} [A_\rho(\dot{\tilde{u}}_1^2 + \dot{\tilde{u}}_2^2) + I_\rho(\dot{\tilde{\alpha}} + \dot{\psi})^2]\,dX_1 \\ + \; & \tfrac{1}{2}\int_{[0,L]} A_\rho\{2\dot{\psi}[-\tilde{u}_2\dot{\tilde{u}}_1 + (X_1+\tilde{u}_1)\dot{\tilde{u}}_2] + \dot{\psi}^2[(X_1+\tilde{u}_1)^2 + \tilde{u}_2^2]\}\,dX_1 \end{aligned}} \tag{2.13}$$

Here, the inertia constants A_ρ and I_ρ are defined as

$$A_\rho := \int_{[-\frac{h}{2},\frac{h}{2}]} \rho(X_1,X_2)\,dX_2, \qquad I_\rho := \int_{[-\frac{h}{2},\frac{h}{2}]} \rho(X_1,X_2)\,X_2^2\,dX_2 \tag{2.14}$$

2.4. Equations of motion: Coupled inertia terms

The equations of motion governing the dynamical system under consideration may be systematically derived from the expressions for the kinetic and potential energies by means of Hamilton's principle. Accordingly, we require that the action

$$\int_{[t_1,t_2]} (K - \Pi)\,dt \quad \text{be stationary} \tag{2.15}$$

for arbitrary paths connecting two points at time t_1 and t_2 in the configuration space. By substituting expressions (2.5) and (2.13) into (2.14) and making use of standard arguments involving integration by parts, we arrive at the following equations governing the extensional and flexural motion of the beam

$$\begin{aligned} A_\rho[\ddot{\tilde{u}}_1 - \ddot{\psi}\tilde{u}_2 - 2\dot{\psi}\dot{\tilde{u}}_2 - \dot{\psi}^2(X_1+\tilde{u}_1)] \; - \; & EA\,\tilde{u}''_1 = 0 \\ A_\rho[\ddot{\tilde{u}}_2 + \ddot{\psi}(X_1+\tilde{u}_1) + 2\dot{\psi}\dot{\tilde{u}}_1 - \dot{\psi}^2\tilde{u}_2)] \; - \; & GA_s(\tilde{u}'_2 - \tilde{\alpha}) = 0 \\ I_\rho(\ddot{\tilde{\alpha}} + \ddot{\psi}) \; - \; & EI\,\tilde{\alpha}'' - GA_s(\tilde{u}'_2 - \tilde{\alpha}) = 0 \end{aligned} \tag{2.16}$$

Appropriate boundary conditions automatically follow from the argument (see, e.g., Fung [1965]). In addition to the basic balance equations (2.16), one obtains the following equation that expresses the overall balance of angular momentum of the system

$$\begin{aligned} & \ddot{\psi}[\tilde{u}_2^2 + (X_1+\tilde{u}_1)^2] + 2\dot{\psi}[\dot{\tilde{u}}_1(X_1+\tilde{u}_1) + \dot{\tilde{u}}_2\tilde{u}_2] \\ & - \tilde{u}_2\ddot{\tilde{u}}_1 + (X_1+\tilde{u}_1)\ddot{\tilde{u}}_2 + I_\rho(\ddot{\psi}+\ddot{\tilde{\alpha}})^2 = T(t) \end{aligned} \tag{2.17}$$

The highly nonlinear nature of the coupled system (2.16)-(2.17) involving the variables $\{\tilde{u}_1, \tilde{u}_2, \tilde{\alpha}, \psi\}$ should be noted.

Remark 2.1. The variable $\tilde{\alpha}$ can be eliminated from the equations of motion (2.16) by raising the order of the spatial derivatives appearing in the resulting equations. The procedure is analogous to that discussed in Remark 2.2. •

Remark 2.2. The Euler-Bernoulli (constrained) formulation is obtained from the above equations by assuming that *shear deformation is negligible*. Accordingly, one lets

$$(\tilde{u}'_2 - \tilde{\alpha}) \to 0, \quad \text{and} \quad GA_s \to \infty, \quad \text{so that} \quad GA_s(\tilde{u}'_2 - \tilde{\alpha}) \to V \tag{2.18}$$

where V is the shear force acting on the cross section of the beam. Equations $(2.16)_{2,3}$ governing the transversal and flexural vibrations of the beam may be combined, and lead to the following equation

$$A_2\ddot{\tilde{u}}_2 + EI\,\tilde{u}''''_2 - I_\rho\ddot{\tilde{u}}''_2 + A_\rho[\ddot{\psi}(X_1+\tilde{u}_1) + 2\dot{\psi}\dot{\tilde{u}}_1 - \dot{\psi}^2\tilde{u}_2)] = 0 \qquad (2.19)$$

We note that the first two terms in (2.19) correspond to the standard *linear* Euler-Bernoulli beam theory. The third one gives the contribution of the *rotatory inertia* and is often neglected in most structural applications. The last three terms within brackets arise as a result of coupling between deformation and rigid body motion. These terms represent the *inertia due to rotation of the shadow beam*, the *Coriolis* and the *centrifugal* effects, respectively. ▪

3. Proposed approach based on finite strains: Inertial frame.

The introduction of the floating frame, although simplying the expression of the stiffness part of the equations of motion, results in a complex nonlinear coupled structure of the inertia terms. In some sense, the approch proposed in this section is based on the opposite philosophy. Here, the structure of the inertia operator is simplified to the standard *linear uncoupled* case simply by referring the basic equations of motion to the *inertial* frame. This results in a drastic simplification of the inertia (temporal) part, the nonlinearity now being shifted to the stiffness (spatial) part of the equations of motion. Conceptually, the essential step needed in developing this alternative approach is the use of rod theories capable of accounting for large rotations. In section 3.3, we summarize from a physical standpoint the appropriate strain measures of a model of this kind, essentially due to Reissner [1972]. For the three dimensional version, we refer to Antman [1974], Simo [1985], and Simo & Vu Quoc [1985]. An essential characteristic of these strain measures is their *invariance under superposed rigid body motions*.

From a computational standpoint, the substantial advantage of the proposed approach over the shadow beam approach discussed in Section 2 lies in a much simpler structure of the resulting equations. This structure corresponds to the standard nonlinear system of ODE's that typically arises in nonlinear structural dynamics. In addition, we automatically account for large strains.

3.1. Basic kinematic assumption.

As in Section 2, the basic kinematic assumption is the condition that plane sections normal to axis of the beam in the undeformed configuration remain plane; i.e.,

$$\boldsymbol{\phi}(X_1, X_2, t) := \boldsymbol{\phi}_0(X_1, t) + X_2\,\mathbf{t}_2(X_1, t) \qquad (3.1a)$$

The difference between assumptions (2.1a) and (3.1a) is that the position vector $\boldsymbol{\phi}_0$ and the moving vectors $\{\mathbf{t}_1, \mathbf{t}_2\}$ following the deformation of the beam are now expressed relative to the *inertial frame* $\{\mathbf{e}_1, \mathbf{e}_2\}$. Accordingly, we set

$$\begin{aligned}
\boldsymbol{\phi}_0(X_1, t) &:= [X_1 + u_1(X_1, t)]\,\mathbf{e}_1 + u_2(X_1, t)\,\mathbf{e}_2 \\
\mathbf{t}_1(X_1, t) &:= \cos\vartheta(X_1, t)\,\mathbf{e}_1 + \sin\vartheta(X_1, t)\,\mathbf{e}_2 \\
\mathbf{t}_2(X_1, t) &:= -\sin\vartheta(X_1, t)\,\mathbf{e}_1 + \cos\vartheta(X_1, t)\,\mathbf{e}_2
\end{aligned} \qquad (3.1b)$$

As in (2.2) we shall use matrix notation and express relations $(3.1b)_{2,3}$ as

$$\begin{Bmatrix}\mathbf{t}_1\\ \mathbf{t}_2\end{Bmatrix} = \Lambda^t \begin{Bmatrix}\mathbf{e}_1\\ \mathbf{e}_2\end{Bmatrix}, \quad \text{where} \quad \Lambda := \begin{bmatrix}\cos\vartheta & -\sin\vartheta\\ \sin\vartheta & \cos\vartheta\end{bmatrix} \qquad (3.2)$$

Remark 3.1. It should be noted that the floating basis $\{\mathbf{a}_1, \mathbf{a}_2\}$ is entirely by-passed and plays no role in the present formulation. ▪

3.2. Motivation: Kinetic energy

The direct use of the inertial frame $\{\mathbf{e}_1, \mathbf{e}_2\}$ in the formulation of the dynamics of the system is motivated by the form taken by the kinetic energy. As shown below, relative to the inertial basis, the kinetic energy of the system reduces to the standard *quadratic uncoupled* form. To see this, note that from (3.2) the rate of change of the moving vectors $\{\mathbf{t}_1, \mathbf{t}_2\}$ is given by

$$\dot{\mathbf{t}}_1 = \dot{\vartheta}\mathbf{t}_2, \qquad \dot{\mathbf{t}}_2 = -\dot{\vartheta}\mathbf{t}_1 \tag{3.4}$$

Hence, the time derivative $\dot{\boldsymbol{\phi}}$ of the position vector $\boldsymbol{\phi}$ is given simply as

$$\begin{aligned} \dot{\boldsymbol{\phi}} &= \dot{\boldsymbol{\phi}}_0 - X_2\dot{\vartheta}\mathbf{t}_1 \\ \dot{\boldsymbol{\phi}}_0 &= \dot{u}_1\mathbf{e}_1 + \dot{u}_2\mathbf{e}_2 \end{aligned} \tag{3.5}$$

It follows from (3.5) that $\|\dot{\boldsymbol{\phi}}\|^2 := \dot{\varphi}_1^2 + \dot{\varphi}_2^2$ has the expression

$$\|\dot{\boldsymbol{\phi}}\|^2 = [\dot{u}_1^2 + \dot{u}_2^2] + X_2^2\dot{\vartheta}^2 - 2\dot{\vartheta}X_2(\cos\vartheta\dot{u}_1 + \sin\vartheta\dot{u}_2) \tag{3.6}$$

Upon integrating $\rho(X_1, X_2)\|\dot{\boldsymbol{\phi}}\|^2$ over $[0, L]\times[-\frac{h}{2}, \frac{h}{2}]$, we arrive at the following expression for the kinetic energy of the system

$$\boxed{K \equiv \tfrac{1}{2}\int_{[0,L]} [A_\rho(\dot{u}_1^2 + \dot{u}_2^2) + I_\rho\dot{\vartheta}^2]\,dX_1} \tag{3.7a}$$

Here, as in (2.13), the inertia coefficients A_ρ and I_ρ are given by (2.14).

Remark 3.2. The case of a flexible beam attached to a rigid body, e.g., see Levinson & Kane [1981], can be readily accounted for within the present formulation by modifying expression (3.7a) for the kinetic energy as follows. Let m_R be the mass of the rigid body, and I_R its inertia relative to an axis parallel to $\mathbf{e}_3 \equiv \mathbf{t}_3$ and passing through the connecting point with the beam. The kinetic energy of the composite system, then, is given by

$$K_{total} = K + \tfrac{1}{2}m_R\|\dot{\boldsymbol{\phi}}_0(0, t)\|^2 + \tfrac{1}{2}I_R\dot{\vartheta}^2(0, t) \tag{3.7b}$$

where K is given by (3.7a). ▪

Remark 3.3. It is noted that expression (2.13) for the kinetic energy in the shadow beam approach may be *exactly* recovered from (3.7) simple by employing the coordinate transformation

$$\begin{Bmatrix} X_1 + u_1 \\ u_2 \end{Bmatrix} = \begin{bmatrix} \cos\psi & -\sin\psi \\ \sin\psi & \cos\psi \end{bmatrix} \begin{Bmatrix} X_1 + \tilde{u}_1 \\ \tilde{u}_2 \end{Bmatrix} \tag{3.8}$$

That is, the expression for the kinetic energy of the system is independent of any particular assumption on the magnitude of the strain field. ▪

Next, we discuss the appropriate expression for the potential energy of the system.

3.3. Potential energy: Invariant strain measures.

Within the context of large strains, a physically reasonable definition of the strain field in the beam is also provided in vectorial form by expression (2.4); i.e.,

$$\boldsymbol{\gamma} := \boldsymbol{\phi}'_0 - \mathbf{t}_1, \qquad \boldsymbol{\kappa} := \vartheta'\mathbf{t}_3 \tag{3.9a}$$

The physical interpretation of γ is clear as shown in Figure 3.1. γ measures the difference between the slope of the deformed axis of the beam and the normal to the cross section defined by $\mathbf{t}_1$, and κ is the rate of rotation of the cross section along the undeformed length of the beam. In component form, relative to the inertial frame we have from (3.1b) the following expression for γ

$$\gamma = \gamma_1 \mathbf{e}_1 + \gamma_2 \mathbf{e}_2 \equiv [(1 + u'_1) - \cos\vartheta]\mathbf{e}_1 + [u'_2 - \sin\vartheta]\mathbf{e}_2 \qquad (3.9b)$$

Alternatively, relative to the *moving vectors* $\{\mathbf{t}_1, \mathbf{t}_2\}$, from relation (3.2) we have the following expression

$$\gamma = \Gamma_1 \mathbf{t}_1 + \Gamma_2 \mathbf{t}_2 \qquad (3.10a)$$

where

$$\boxed{\begin{Bmatrix}\Gamma_1 \\ \Gamma_2\end{Bmatrix} = \Lambda^t \begin{Bmatrix}1 + u'_1 - \cos\vartheta \\ u'_2 - \sin\vartheta\end{Bmatrix}} \qquad (3.10b)$$

The parallelism between expressions (2.4a,b,c) and (3.9a)-(3.9b) should be noted. We now assume that relative to the moving frame $\{\mathbf{t}_1, \mathbf{t}_2\}$ we have the same expression for the potential energy as the one considered in the small strain shadow beam approach discussed in Section 2. Accordingly, we set

$$\Pi := \tfrac{1}{2} \int_{[0,L]} \{EA\,\Gamma_1^2 + GA_s\,\Gamma_2^2 + EI\,\vartheta'^2\}\,dS + \Pi_{EXT} - T(t)\,\vartheta(0,t) \qquad (3.11)$$

Remark 3.4. It is essential to note that the components of the strain γ in the basis $\{\mathbf{t}_1, \mathbf{t}_2\}$ denoted by $[\Gamma_1 \quad \Gamma_2]^t$ are *invariant under superposed rigid body motions* on the beam. One can see this by considering the rigid body motion composed of a superposed translation $\mathbf{c}(t)$, and a superposed rotation $\beta(t)$ represented by the orthogonal transformation matrix

$$\mathbf{Q}(t) := \begin{bmatrix}\cos\beta & -\sin\beta \\ \sin\beta & \cos\beta\end{bmatrix} \qquad (3.12a)$$

The transformed quantities in the expression of Γ_i in (3.10) above are as follows

$$\boldsymbol{\phi}_0^+(X_1,t) = \mathbf{c}(t) + \mathbf{Q}(t)\,\boldsymbol{\phi}_0(X_1,t)\,; \quad \boldsymbol{\phi}_0^{+\prime} := \phi_{01}^{+\prime}\mathbf{e}_1 + \phi_{02}^{+\prime}\mathbf{e}_2 = \mathbf{Q}\boldsymbol{\phi}_0', \qquad (3.12b)$$

$$\text{i.e.,} \quad \begin{Bmatrix}\phi_{01}^{+\prime} \\ \phi_{02}^{+\prime}\end{Bmatrix} = \mathbf{Q}\begin{Bmatrix}1 + u'_1 \\ u'_2\end{Bmatrix}, \qquad (3.12c)$$

$$\Lambda^+ = \mathbf{Q}\Lambda, \qquad (3.12d)$$

$$\mathbf{t}_1^+ = \cos(\beta+\vartheta)\,\mathbf{e}_1 + \sin(\beta+\vartheta)\,\mathbf{e}_2\,. \qquad (3.12e)$$

As a result, one can immediately see that

$$\gamma^+ := \Gamma_1^+ \mathbf{t}_1^+ + \Gamma_2^+ \mathbf{t}_2^+ = \boldsymbol{\phi}_0^{+\prime} - \mathbf{t}_1^+ \qquad (3.13a)$$

where

$$\begin{Bmatrix}\Gamma_1^+ \\ \Gamma_2^+\end{Bmatrix} = \Lambda^{+t}\left[\begin{Bmatrix}\phi_{01}^{+\prime} \\ \phi_{02}^{+\prime}\end{Bmatrix} - \begin{Bmatrix}\cos(\beta+\vartheta) \\ \sin(\beta+\vartheta)\end{Bmatrix}\right] \equiv \begin{Bmatrix}\Gamma_1 \\ \Gamma_2\end{Bmatrix} \qquad (3.13b)$$

The invariance under superposed rigid body motions of the *curvature* κ follows at once in the plane case from expression (3.9a). This invariance property of the

strain measures is essential for the success of the proposed approach. ▪

Remark 3.5. It can be shown that definition (3.9a) and expressions (3.9b), (3.10) indeed follow from a rigorous argument based on the equivalence of the stress power for the general three dimensional theory with the reduced stress power of the (finite strain) beam theory. We refer to Simo [1985] and, in a different context, to Antman [1972,1974]. ▪

Remark 3.6. In this paper, we shall be concerned only with *spatially fixed* load, which does not depend on the deformed configuration, as opposed to *follower* load. The latter is configuration dependent. For a treatment of follower loads in the general context of the three-dimensional finite strain beam we refer to Simo & Vu Quoc [1985]. Accordingly, the potential of the distributed loading in $(0, L)$ is given by

$$\Pi_{EXT} = \int_{[0,L]} [\bar{\mathbf{m}} \cdot \vartheta \mathbf{e}_3 + \bar{\mathbf{n}} \cdot \boldsymbol{\phi}_0] dX_1 \tag{3.13c}$$

Here, $\bar{\mathbf{n}}(X_1, t) := \bar{n}_1(X_1, t)\mathbf{e}_1 + \bar{n}_2(X_1, t)\mathbf{e}_2$ and $\bar{\mathbf{m}}(X_1, t) := \bar{m}(X_1, t)\mathbf{e}_3$ are the external force and torque per unit of reference length acting on the beam. ▪

3.4. Equations of motion: Uncoupled inertia terms.

As in Section 2, one may obtain systematically the equations of motion governing the evolution of the system by employing Hamilton's principle. Standard manipulation yields the following result

$$A_\rho \ddot{\boldsymbol{\phi}}_0 - [\boldsymbol{\Lambda}\mathbf{C}\boldsymbol{\Lambda}^t \begin{Bmatrix} 1 + u'_1 - \cos\vartheta \\ u'_2 - \sin\vartheta \end{Bmatrix}]' - \bar{n} = 0 \tag{3.14a}$$

$$I_\rho \ddot{\vartheta} - EI\vartheta'' - \begin{Bmatrix} -u'_2 \\ 1 + u'_1 \end{Bmatrix}^t \boldsymbol{\Lambda}\mathbf{C}\boldsymbol{\Lambda}^t \begin{Bmatrix} 1 + u'_1 - \cos\vartheta \\ u'_2 - \sin\vartheta \end{Bmatrix} - \bar{m} = 0 \tag{3.14b}$$

We recall that $\boldsymbol{\Lambda}$ and $\mathbf{C}$ are given by

$$\mathbf{C} := \begin{bmatrix} EA & 0 \\ 0 & GA_s \end{bmatrix}, \qquad \boldsymbol{\Lambda} := \begin{bmatrix} \cos\vartheta & -\sin\vartheta \\ \sin\vartheta & \cos\vartheta \end{bmatrix} \tag{3.14c}$$

Equations (3.14a,b) comprise the system of nonlinear partial differential equations governing the evolution of the system. Note that although (3.14) are nonlinear, these equations are *linear in the time derivative terms*. To define the *natural* boundary conditions, and for subsequent developments, we introduce the notation

$$\begin{Bmatrix} n_1 \\ n_2 \end{Bmatrix} := \boldsymbol{\Lambda}\mathbf{C}\boldsymbol{\Lambda}^t \begin{Bmatrix} 1 + u'_1 - \cos\vartheta \\ u'_2 - \sin\vartheta \end{Bmatrix}, \qquad m := EI\vartheta' \tag{3.15}$$

Here, $\mathbf{n}(X_1, t) := n_1(X_1, t)\mathbf{e}_1 + n_2(X_1, t)\mathbf{e}_2$ and $\mathbf{m}(X_1, t) := m(X_1, t)\mathbf{e}_3$ represent the *internal force* and *internal moment* acting on a deformed cross section of the beam. According to our model problem, we assume the following natural boundary conditions

$$\mathbf{m}(0, t) = T(t)\mathbf{e}_3, \quad \mathbf{m}(L, t) \equiv \mathbf{n}(0, t) \equiv \mathbf{n}(L, t) \equiv \mathbf{0} \tag{3.16}$$

These boundary conditions follow automatically from Hamilton's principle and the appropriate expression of Π_{EXT}. ▪

3.5. Conservation of global momenta.

It is noted that within the proposed approach *global* linear and angular momenta are automatically satisfied, and *do not* provide any additional condition. This is in contrast with the shadow beam approach in which the basic equations of motion (2.16) must be supplemented by the global angular momentum condition (2.17) for the evolution of the system to be completely determined.

To see that satisfaction of *global* linear and angular momenta is ensured in the present approach, we start by rewritting equations (3.14a,b) with the aid of (3.16) simply as

$$\dot{\mathbf{L}} - \mathbf{n}' - \bar{\mathbf{n}}' = \mathbf{0}, \quad \dot{\mathbf{H}} - \mathbf{m}' - \boldsymbol{\phi}'_0 \times \mathbf{n} - \bar{\mathbf{m}} = \mathbf{0} \tag{3.17a}$$

Here $\mathbf{L}(X_1, t)$ denotes the linear momentum per unit of deformed length, given by

$$\mathbf{L} := \int_{[-\frac{h}{2}, \frac{h}{2}]} \rho \boldsymbol{\phi} \, dX_2 = A_\rho \dot{\boldsymbol{\phi}}_0, \tag{3.17b}$$

where use has been made of (3.1a). In addition $\mathbf{H}(X_1, t)$ is the angular momentum per unit length, relative to the centroid of the deformed cross section, thus given by

$$\mathbf{H} := \int_{[-\frac{h}{2}, \frac{h}{2}]} \rho [\boldsymbol{\phi} - \boldsymbol{\phi}_0] \times \dot{\boldsymbol{\phi}} \, dX_2 = I_\rho \dot{\vartheta} \tag{3.17c}$$

The *global* linear and angular momentum of the system denoted by $\mathbb{L}(t)$ and $\mathbb{H}(t)$, respectively, are defined as

$$\mathbb{L}(t) := \int_{[0,L]\times[-\frac{h}{2}, \frac{h}{2}]} \rho \dot{\boldsymbol{\phi}} \, dX_1 dX_2, \qquad \mathbb{H}(t) := \int_{[0,L]\times[-\frac{h}{2}, \frac{h}{2}]} \rho \boldsymbol{\phi} \times \dot{\boldsymbol{\phi}} \, dX_1 dX_2 \tag{3.18}$$

By making use of the identity $\boldsymbol{\phi} \times \dot{\boldsymbol{\phi}} = (\boldsymbol{\phi} - \boldsymbol{\phi}_0) \times \dot{\boldsymbol{\phi}} + \boldsymbol{\phi}_0 \times \dot{\boldsymbol{\phi}}$, it follows that the global angular momentum may be expressed simply as

$$\mathbb{H}(t) = \int_{[0,L]} [\mathbf{H} + \boldsymbol{\phi}_0 \times \mathbf{L}] \, dX_1 \tag{3.19}$$

where $\mathbf{L}(X_1, t)$ and $\mathbf{H}(X_1, t)$ are defined by (3.17b,c). By time differentiating (3.19) and by making use of (3.17a), we arrive at the following condition involving the applied load and boundary conditions

$$\dot{\mathbb{H}} = [\mathbf{m} + \boldsymbol{\phi}_0 \times \mathbf{n}] \Big|_{X_1=0}^{X_1=L} + \int_{[0,L]} [\bar{\mathbf{m}} + \boldsymbol{\phi}_0 \times \bar{\mathbf{n}}] \, dX_1 \tag{3.20}$$

Condition (3.20) simply states that the resultant torque of the applied loading equals the rate of change of the total angular momentum, in agreement with Euler's second law of motion. Similarly, for the global linear momentum we obtain

$$\dot{\mathbb{L}} = \mathbf{n} \Big|_{X_1=0}^{X_1=L} + \int_{[0,L]} \bar{\mathbf{n}} \, dX_1 \tag{3.21}$$

which states that the resultant force of the applied load equals the rate of change of the global linear momentum.

Remark 3.7. Equations of motion (3.17a) along with definitions (3.17b) and (3.17c) are general, and remain valid in the three dimensional theory. Thus, the foregoing discussion leading to expressions (3.20) and (3.21) is general and not restricted to the plane case. ▪

4. Numerical approximation: Galerkin method.

In this section we discuss the numerical treatment of the nonlinear partial differential equations developed in Section 3. The basic strategy is to perform a Galerkin discretization in the spatial variable leading to the standard system of ODE's in the time variable characteristic of nonlinear structural dynamics. This system may then be treated by standard time stepping algorithms such as the Newmark family. The finite element method provides an established and well understood technique for constructing the (spatial) basis functions necessary to performed the Galerkin discretization. Expressions of the matrices resulting from the application of this procedure are given in the appendix.

4.1. Weak form of equations of motion —Spatial discretization.

The equations of motion (3.14) may be put in the following form

$$\mathbf{I}\,\ddot{\mathbf{d}}(X_1,t) + \mathbb{P}[\mathbf{d}(X_1,t)] = \mathbf{f}(X_1,t), \tag{4.1a}$$

where

$$\mathbf{I} := Diag[A_\rho, A_\rho, I_\rho],$$
$$\mathbf{d}(X_1,t) := \begin{Bmatrix} X_1 + u_1(X_1,t) \\ u_2(X_1,t) \\ \vartheta(X_1,t) \end{Bmatrix}, \qquad \mathbf{f}(X_1,t) := \begin{Bmatrix} \bar{n}_1(X_1,t) \\ \bar{n}_2(X_1,t) \\ \bar{m}(X_1,t) \end{Bmatrix} \tag{4.1b}$$

Equation (4.1a) is a nonlinear partial differential equation in the generalized vector $\mathbf{d}(X_1,t)\in V_1$, where V_1 is the space of admissible (generalized) displacements. † This equation is linear in the term involving time derivative, i.e. the acceleration $\ddot{\mathbf{d}}$ in the first term. The second term $\mathbb{P}[\mathbf{d}]$, on the other hand, is a non-linear differential operator in the space variable $X_1\in(0,L)$. The nonlinear nature of this term is the result of the coupling between large overall motions and (finite) strain deformations in the beam. Concerning the applied load $\bar{\mathbf{n}}$ and $\bar{m}$, see remark 3.5. The weak form $G(\mathbf{d},\eta)$ of equation (4.1a) is obtained by integrating over the spatial domain $(0,L)\subset\mathbb{R}$ the dot product of this equation with an arbitrary weighting function $\eta\in V_2$. ‡ That is

$$G(\mathbf{d},\eta) := \int_{[0,L]} \eta^t[\mathbf{I}\,\ddot{\mathbf{d}} + \mathbb{P}[\mathbf{d}] - \mathbf{f}]dX_1 = 0, \quad \forall\,\eta\in V_2 \tag{4.2}$$

The final expression is obtained from (4.2) by integration by parts on the spatial derivatives entering $\mathbb{P}[\mathbf{d}]$, so that only *first order spatial derivatives* are involved in $G(\mathbf{d},\eta)$. we refer to the appendix for the details. The displacements $\mathbf{d}(X_1,t)$ and the weighting function $\eta(X_1)$ are then interpolated in the spatial variable X_1 according to

$$\mathbf{d}(X_1,t) \cong \sum_{I=1}^{N} \Psi_I(X_1)\,\mathbf{q}_I(t), \qquad \eta(X_1) \cong \sum_{I=1}^{N} \Psi_I(X_1)\,\eta_I^b \tag{4.3}$$

Upon introducing the spatial discretization (4.3) of $\mathbf{d}(X_1,t)$ and of $\eta(X_1)$ into the weak form (4.2), we obtain the semi-discrete equation of motion in matrix form

† A possible choice for V_1 could be $V_1 := \{\mathbf{d}\in(H^1[0,L]\times C^\infty[0,\infty))^3\}$.
‡ V_2 could be chosen to be $V_2 := \{\eta\in(H^1[0,L])^3 \mid \eta^t[n_1, n_2, m]^t\big|_{X_1=0}^{X_1=L} = 0\}$.

$$\boxed{\mathbf{M}\ddot{\mathbf{q}}(t) + \mathbf{P}(\mathbf{q}(t)) = \mathbf{F}(t)} \tag{4.4}$$

where $\mathbf{M}$ represents the mass matrix, $\mathbf{q}(t) := [\,\mathbf{q}_1(t), \ldots, \mathbf{q}_N(t)\,]^t$ the generalized displacements, $\mathbf{P}(\mathbf{q}(t))$ the internal forces, which is non-linear in $\mathbf{q}(t)$, and $\mathbf{F}(t)$ the applied load. Details of the expressions of $\mathbf{M}$, $\mathbf{P}(\mathbf{q}(t))$, and $\mathbf{F}(t)$ can be found in the appendix.

Remark 4.1. For the case at hand where the system has a well defined energy function $H = K + \Pi$, the Galerkin procedure outlined above is equivalent to a standard Raleigh-Ritz approximation based on $(4.3)_1$. See, e.g., Meirovitch [1967]. ▪

Remark 4.2. In the shadow beam approach restricted to small-strains , one may also use the modal superposition method to discretize spatially the displacements $[\tilde{u}_1, \tilde{u}_2]$ as in (4.3). As noted in Remark 2.1, this can be done by first eliminating $\tilde{\alpha}$ from (2.16) using $(2.16)_2$. The semi-discrete equation of motion of the system is then obtained by projecting the resulting equations (2.16) onto the orthogonal basis of mode-shapes of the Euler-Bernoulli cantilever beam. However, no matter what the discretization procedure may be, the resulting semi-discrete equation of motion is a system of highly *coupled non-linear differential algebraic equations* (DAE). The solution of this complete system of DAE's is not a trivial task, and requires a specially designed computer code (see, e.g., Benson & Hallquist [1985]). On the numerical methods to solve a system of DAE's, we refer to Gear [1971a,b], Petzold [1982], Gear & Petzold [1984]. The solution of the standard non-linear structural dynamics equation (4.4) is, by contrast, much simpler, and may be carried out on any non-linear structural finite element code. The time stepping algorithm for this solution procedure will be outlined in the next section. ▪

Remark 4.3. Multibody dynamics. In section 5, we will show through numerical examples that the proposed approach can be immediately applied to study the dynamics of a system of flexible bodies connected through hinges without alteration in the formulation. It is indeed a simple matter to model such a system in a finite element code. The shadow beam approach, on the other hand, leads to a much more involved formulation (see, e.g., Likins [1974b], Hughes [1979], Song & Haug [1980], Sunada & Dubowsky [1980]) ▪

4.2. Time stepping scheme —Temporal discretization.

The *semi-discrete* equations of motion (4.4) can be trivially rephrased into the *standard form of a system of non-linear ODE's*, $\dot{\mathbf{y}} = \mathbf{g}(\mathbf{y},t)$, simply by setting $\mathbf{y} := \{\mathbf{q}, \dot{\mathbf{q}}\}$. This standard ODE system can be integrated by a variety of time stepping algorithms; see e.g. Gear [1971a], which must be *consistent* with (4.4) and *stable* for some range of the time step. We refer to standard textbooks, e.g., Richtmyer & Morton [1967] or Gear [1971a] for precise definitions of these concepts. Two basic strategies in devising algorithms for (4.4) may be adopted

(a) *Explicit schemes*: Typically high accuracy may be achieved by employing high order methods. A classical example is furnished by the family of Runge-Kutta methods. The main drawback of explicit schemes is their restrictive stability characteristics that impose severe limitations on the time step.

(b) *Implicit schemes* typically possess very robust stability characteristics. Classical examples are the trapezoidal rule, which is the highest order possible A-stable method (Dahlquist [1963]), the Gear's stiffly stable methods (Gear [1971a]), and the Newmark family of algorithms (Newmark [1959]) widely used in nonlinear structural dynamics, (see e.g., Belytschko &

Hughes [1983]).

Here, motivated for stability considerations, attention is focussed on the Newmark family of algorithms for solving (4.4), which includes the trapezoidal rule as a special case. The theoretical analysis of the behavior of Newmark's algorithm in the linear case is well established; see e.g. Hilber [1976]. In the remaining of this section, for completeness, we outline the basic steps involved in the numerical solution of (4.4) by the Newmark algorithm.

Let $\mathbf{q}_n$ denote the approximated solution to $\mathbf{q}(t_n)$ at time t_n. Similarly, $\mathbf{v}_n \cong \dot{\mathbf{q}}(t_n)$ and $\mathbf{r}_n \cong \ddot{\mathbf{q}}(t_n)$ represent the approximated velocity and acceleration at time t_n, respectively. Assume that the solution $\{\mathbf{q}_n, \mathbf{v}_n, \mathbf{r}_n\}$ at time t_n has already been obtained, i.e., the momentum equation (4.4) is satisfied at time t_n

$$\mathbf{M}\mathbf{r}_n + \mathbf{P}(\mathbf{q}_n) = \mathbf{F}_n \tag{4.5}$$

where $\mathbf{F}_n \equiv \mathbf{F}(t_n)$. We now aim at satisfying the momentum equation (4.4) at time t_{n+1}, i.e.,

$$\mathbf{M}\mathbf{r}_{n+1} + \mathbf{P}(\mathbf{q}_{n+1}) = \mathbf{F}_{n+1} \tag{4.6}$$

The Newmark time stepping algorithm defines the relationship between $\{\mathbf{q}_{n+1}, \mathbf{v}_{n+1}, \mathbf{r}_{n+1}\}$ according to the following formulae

$$\mathbf{r}_{n+1} = \frac{\mathbf{q}_{n+1} - \mathbf{q}_n}{h^2\beta} - \frac{\mathbf{v}_n}{h\beta} - \frac{\frac{1}{2} - \beta}{\beta}\mathbf{r}_n \tag{4.7a}$$

$$\mathbf{v}_{n+1} = \mathbf{v}_n + h[(1-\tau)\mathbf{r}_n + \tau\mathbf{r}_{n+1}], \tag{4.7b}$$

where $h := t_{n+1} - t_n$ denotes the time step size, and (β, τ) are the parameters of the Newmark algorithm. Recall that $\beta = 0.25$ and $\tau = 0.5$ correspond to the trapezoidal rule; this choice of the parameters β and τ renders the algorithm *unconditionally stable*, †† and second order accurate. Substitution of (4.7a) into (4.6) yields a system of non-linear algebraic equations in terms of $\mathbf{q}_{n+1}$.

The resulting non-linear algebraic system may then be solved employing the classical iterative Newton-Raphson method. Let $\mathbf{q}_{n+1}^{(i)}$ denote the value of $\mathbf{q}_{n+1}$ at iteration (i) of the Newton-Raphson algorithm, and $\Delta\mathbf{q}_{n+1}^{(i+1)}$ the incremental displacements. As an initial guess of the value of $\{\mathbf{q}_{n+1}, \mathbf{v}_{n+1}, \mathbf{r}_{n+1}\}$, one may choose the starting value $\mathbf{q}_{n+1}^{(0)}$ to be the same as the converged one in the previous time increment, i.e. $\mathbf{q}_n$; the initial values $\mathbf{v}_{n+1}^{(0)}$ and $\mathbf{r}_{n+1}^{(0)}$ follow from the Newmark scheme (4.7):

$$\mathbf{q}_{n+1}^{(0)} = \mathbf{q}_n \tag{4.8a}$$

$$\mathbf{r}_{n+1}^{(0)} = -\left[\frac{\mathbf{v}_n}{h\beta} + \frac{\frac{1}{2} - \beta}{\beta}\mathbf{r}_n\right] \tag{4.8b}$$

$$\mathbf{v}_{n+1}^{(0)} = \mathbf{v}_n + h[(1-\tau)\mathbf{r}_n + \tau\mathbf{r}_{n+1}^{(0)}] \tag{4.8c}$$

At iteration (i) of the Newton-Raphson scheme, the linearization about $\mathbf{q}_{n+1}^{(i)}$ of the above system of non-linear algebraic equations yields

$$\left[\frac{1}{h^2\beta}\mathbf{M} + \mathbf{K}_T(\mathbf{q}_{n+1}^{(i)})\right]\Delta\mathbf{q}_{n+1}^{(i+1)} = \mathbf{F}_{n+1} - \mathbf{M}\mathbf{r}_{n+1}^{(i)} - \mathbf{P}(\mathbf{q}_{n+1}^{(i)}) \tag{4.9}$$

†† Roughly, the notion of stability corresponds to well-posedness of the semi-discrete problem. In the nonlinear case, several notions of stability have been proposed (A-stability, spectral stability, stiffly-stable methods,... etc.). See, e.g., Gear [1971a] or Belytschko & Hughes [1983].

It should be noted here that while the mass matrix $\mathbf{M}$ is positive definite, the tangent stiffness matrix $\mathbf{K}_t(\mathbf{q}_{n+1}^{(i)})$ may be positive semi-definite. The system of equations (4.9) is of the form $\widehat{\mathbf{K}}\Delta\mathbf{q}_{n+1}^{(i+1)} = \widehat{\mathbf{F}}$ where the matrix $\widehat{\mathbf{K}}$ is banded, symmetric, and positive definite. Solving for $\Delta\mathbf{q}_{n+1}^{(i+1)}$, and updating $(\mathbf{q}_{n+1}^{(i)}, \mathbf{v}_{n+1}^{(i)}, \mathbf{r}_{n+1}^{(i)})$, we obtain the value of $\{\mathbf{q}_{n+1}, \mathbf{v}_{n+1}, \mathbf{r}_{n+1}\}$ at iteration $(i+1)$ as follows

$$\mathbf{q}_{n+1}^{(i+1)} = \mathbf{q}_{n+1}^{(i)} + \Delta\mathbf{q}_{n+1}^{(i+1)} \tag{4.10a}$$

$$\mathbf{v}_{n+1}^{(i+1)} = \mathbf{v}_{n+1}^{(i)} + \frac{\tau}{h\beta}\Delta\mathbf{q}_{n+1}^{(i+1)} \tag{4.10b}$$

$$\mathbf{r}_{n+1}^{(i+1)} = \mathbf{r}_{n+1}^{(i)} + \frac{1}{h^2\beta}\Delta\mathbf{q}_{n+1}^{(i+1)} \tag{4.10c}$$

The iterations are continued until convergence is attained within certain tolerance. A basic characteristic of Newton's iterative method is that the asymptotic rate of convergence is quadratic.

5. Numerical simulations.

In this section we present a series of numerical simulations that illustrate the formulation and numerical procedure discussed in Sections 3 and 4. Our purpose is to exhibit

(a) The simplicity of the numerical procedure. Essentially any existing nonlinear structural finite element dynamics code could be used. Here the computer program FEAP developed by R.L. Taylor and documented in Zienkiewicz [1977, Chap 24] is employed.

(b) The capability of the proposed formulation of automatically handling *finite strains* superposed onto large overall rigid body motions. This includes flexible bodies in free flight.

(c) The immediate applicability of the proposed approach to the dynamics of a system of interconnected flexible bodies without alteration of the formulation.

It is emphasized that no simplification is made in the simulations that follow in the sense that Coriolis and centrifugal effects as well as the inertia effect due to rotation are automatically accounted for. The deformed shapes in all figures reported in this paper are given in the *same* scale as that of the geometry of the beam, i.e., there is no magnification of the structural deformations.

In all simulations reported herein, the trapezoidal rule (Newmark with $\tau = 0.5$ and $\beta = 0.25$) was employed. Numerical operations were performed in double precision in a VAX 11/780 under the Berkeley UNIX version 4.3 operating system.

Example 5.1. Flexible robot arm. This simulation is concerned with the re-positioning of a flexible beam rotating horizontally about a vertical axis passing through one end. The finite element mesh consists of 10 isoparametric elements with linear interpolation functions for both displacement and rotation. To avoid the well known "shear locking" phenomenon, (see, e.g. Zienkiewicz [1977]), a uniformly reduced one point Gauss quadrature is employed to integrate the tangent stiffness and residual. The mass matrix, however, is integrated exactly with two-point Gauss quadrature. Two cases are considered.

5.1.1. Displacement driven flexible robot arm. The geometry, material properties, finite element mesh, as well as the time step size used in the integration are given in Figure 5.1.1.*a*. Here the robot arm is first repositioned to an angle of 1.5 *radians* from its initial position. This is achieved by prescribing the rotation angle $\psi(t) \equiv \vartheta(0, t)$ as a linear function of time, as shown in Figure 5.1.1.*a*;

the sequence of motion during this repositioning stage is depicted in Figure 5.1.1.*b*. Once the rotation angle $\psi(t)$ is fixed at 1.5 *rad* for all time $t \geq 2.5$, the robot arm then undergoes finite vibrations as shown in Figure 5.1.1.*c*.

5.1.2. Force driven flexible robot arm. Here the robot arm is now driven by a prescribed torque $T(t)$ applied at the axis of rotation $\mathbf{e}_3$, as shown in Figure 5.1.2.*a*. The applied torque is removed at time $t = 2.5$; the robot arm then undergoes a torque-free motion. The simulation is terminated after completion of one revolution, as shown in Figures 5.1.2.*b* and 5.1.2.*c*.

Example 5.2. Flying flexible rod. A flexible rod with free ends, initially placed in an inclined position, is subject to a force and a torque applied simultaneously at one end, see Figure 5.2.1.*a*. The applied force and torque are removed at the same time $t = 2.5$, so that the subsequent free flight of the rod exhibit periodic tumbling pattern. Two cases are considered.

5.2.1. Flexible beam in free flight. The motion of the rod during application of loading is shown in Figure 5.2.1.*b*. The stiffness of the rod is low enough as to exhibit finite deformations. A close-up of the first two revolutions is shown in Figure 5.1.3.*c*, while the entire sequence of motion is depicted in Figure 5.2.1.*d*.

5.2.2. The "flying spaghetti." The bending stiffness, EI of the rod is lowered by a factor of 5 relative to the simulation in 5.2.1. This dramatic reduction in stiffness results in the in the sequence of motions depicted in Figure 5.2.2.

Example 5.3. Multi-body dynamics. Two examples will be considered to illustrate the applicability of the present formulation to the dynamics of multibody systems.

5.3.1. Multi-component robot arm. The robot arm considered in example 5.1.1 is in this example stiffer by a factor of 100, and consists now of two flexible components connected together by a hinge. The two-component robot arm is subjected to the same prescribe rotation $\psi(t) \equiv \vartheta(0, t)$ as in Example 5.1.1. The problem data are summarized in Figure 5.3.1.*a*. The sequence of motions is shown in Figures 5.3.1.*b* and 5.3.1.*c*. Note that while the first component vibrates about the stop angle $\psi(t) = 1.5$ *rad* for $t \geq 2.5$, the second one undergoes a complete revolution about the connecting hinge.

5.3.2. Multibody system in free flight. A two-body system consisting of two flexible links connected by a hinge, is initially at an inclined position. The system is set into motion by applying a force and a torque at one end of the lower link, as shown in Figure 5.3.2. The applied loads are subsquently removed at time $t = 0.5$, so that from there on the articulated beam undergoes free flight. The lower link, indicated by the letter A in the Figure, then moves in the same clockwise direction as the applied torque, whereas the upper link, indicated by the letter B, moves in the opposite counter-clockwise direction.

6. Concluding Remarks.

We have presented a new approach to the dynamics of a plane beam under large overall motions. The essence of this approach is the fully nonlinear plane beam theory that can account for finite rotations as well as finite strains. The appropriate strain measures in this beam theory is invariant under superposed rigid body motion; such invariance is the necessary ingredient to the success of the present approach. The motion of the beam is completely referred to the inertial frame. We thus obtain the expression of the inertia term in the equations of motion simply as mass times acceleration. By contrast, in the shadow beam approach, one obtain a nonlinear and highly coupled inertia operator, and

hence a special computer code need be devised to solve the resulting system. In our approach, the inherent nonlinear character of the problem is transferred to the stiffness part of the equations of motion; this results in a form of equations of motion that arises typically in nonlinear structural dynamics. Consequently, the dynamics of flexible beams under large overall motions can be analyzed in any existing nonlinear finite element code. Without alteration in the formulation, one can apply this approach to the dynamics of a system of flexible beams connected by hinges, as shown in two numerical examples. Further, we will address the following points in forthcoming publications:

(i) The methodology presented in this paper can be employed for the dynamic analysis of an earth-orbiting satellite composed of beam elements. However, one must carefully treat separately the far field and the near field to avoid ill-conditioning. The gravitational force field as well as satellite control actuator forces are configuration dependent and require special treatment.

(ii) Conceptually, the proposed approach readily carries over to the fully three dimensional case. This extension depends crucially on a proper treatment of three dimensional finite rotations in both the structural deformations of the beam and in the overall motions. For the static case, such a treatment is available, Simo & Vu Quoc [1985]. The dynamic case, however, warrants a separate treatment.

Acknowledgements

We thank Prof. R.L. Taylor, the developer of FEAP, for his helpful discussions. This work was performed under the auspices of the Air Force Office of Scientific Research, grant No. AFOSR-83-0361. This support as well as the encouragement provided by Profs. K.S. Pister and E. Polak are gratefully acknowledged.

References

Antman, S.S. [1972], "The theory of rod," *Handbuch der Physics*, Vol. VIa/2, Springer, Berlin.

Antman, S.S. [1974], "Kirchhoff's problem for nonlinearly elastic rods," *Quart. J. of Appl. Math.*, Vol. 32, pp. 221-240.

Ashley, H. [1967], "Observation on the dynamic behavior of flexible bodies in orbit," *AIAA J.*, Vol. 5, No. 3, pp. 460-469.

Baghat, B.M., and K.D. Willmert [1973], "Finite element vibrational analysis of planar mechanism," *Mechanisms and Machine Theory*, Vol. 8, pp. 497-516.

Belytschko T., and T.J.R. Hughes [1983], *Computational Methods for Transient Analysis*, Elsevier Science Publishers.

Benson, D.J., and J.O. Hallquist [1985], "A simple rigid body algorithm for structural dynamics program. Part I," *Proc. of the Int. Conf. on Numerical Methods in Engineering Theory and Applications, Swansea*, Ed. by J. Middleton & G.N. Pande, A.A. Balkema Publishers, Netherlands.

Canavin, J.R. and P.W. Likins [1977], "Floating reference frames for flexible spacecrafts," *J. of Spacecraft*, Vol. 14, No. 12, pp. 724-732.

Dahlquist, G. [1963], "A special stability problem for linear multistep methods," *BIT*, Vol. 3, pp. 27-43.

de Veubeke, B.J. [1976], "The dynamics of flexible bodies," *Int. J. of Engineering Sciences*, Vol. 14, pp. 895-913.

Erdman, A.G., and G.N. Sandor [1972], "Kineto-elastodynamics — A review of the state of the art and trends," *Mechanisms and Machine Theory*, Vol. 7, pp. 19-33.

Fung, Y.C. [1965], *Foundations of Solid Mechanics*, Prentice-Hall, Englewood Cliffs, New Jersey.

Gear, C.W. [1971a], "Simultaneous numerical solution of differential-algebraic equations," *IEEE Transaction on Circuit Theory*, Vol. CT-18, No. 1, pp. 89-95.

Gear, C.W. [1971b], *Numerical Initial Value Problems in Ordinary Differential Equations*, Prentice-Hall, Englewood Cliffs, New Jersey.

Gear, C.W. and L.R. Petzold [1984], "ODE methods for the solution of differential/algebraic systems," *SIAM J. Numerical Analysis*, Vol. 21, No. 4, pp. 716-728.

Goldstein, H. [1980], *Classical Mechanics*, Second edition, Addison Wesley, Reading, Massachusetts.

Grotte, P.B., J.C. McMunn, and R. Gluck [1971], "Equations of motion of flexible spacecraft," *J. of Spacecraft and Rockets*, Vol. 8, No. 6, pp. 561-567.

Hilber, H.M. [1976], "Analysis and design of numerical integration methods in structural dynamics," *Earthquake Engineering Research Center, EERC Report No. 76-29*, University of California, Berkeley.

Hughes, P.C. [1979], "Dynamics of a chain of flexible bodies," *The J. of the Astronautical Sciences*, Vol. 27, pp. 359-380.

Kane, T.R., and D.A. Levinson [1981], "Simulation of large motions of nonuniform beams in orbit: Part II — The unrestrained beam," *The J. of the Astronautical Sciences*, Vol. 29, No. 3, pp. 213-244.

Kane, T.R., P.W. Likins, and D.A. Levinson [1983], *Spacecraft Dynamics*, Mc Graw-Hill Book Co., New York.

Kumar, V.K., and P.M. Bainum [1980], "Dynamics of a flexible body in orbit," *J. of Guidance and Control*, Vol. 3, No. 1, pp. 90-91.

Levinson, D.A., and T.R. Kane [1981], "Simulation of large motions of nonuniform beams in orbit: Part I —The cantilever beam," *The J. of the Astronautical Sciences*, Vol. 29, No.3, pp. 245-276.

Likins, P.W. [1974a], "Analytical dynamics and nonrigid spacecraft simulation," *Jet Propulsion Laboratory, Technical Report 32-1593*, California Institute of Technology.

Likins, P.W. [1974b], "Dynamic analysis of a system of hinge connected rigid bodies with nonrigid appendages," *NASA Technical Report 32-1576.*

Laskin, R.A., P.W. Likins, and R.W. Longman [1981], "Dynamical equations of a free-free beam subject to large overall motions," *The J. of the Astronautical Sciences*, Vol. 31, No. 4, pp. 507-528.

Meirovitch, L. [1970], *Analytical Methods in Vibrations*, MacMillan, Toronto, Canada.

Newmark, N.M. [1959], "A method of computation for structural dynamics," *J. of the Engineering Mechanics Division, ASCE*, pp. 67-94.

Petzold, L.R. [1982], "Differential/algebraic equations are not ODE's," *SIAM J. Sci. Stat. Comput.*, Vol. 3, No. 3, pp. 367-384.

Reissner, E. [1972], "On a one dimensional finite strain beam: The plane problem," *J. Appl. Math. Phys.*, Vol. 23, pp. 795-804.

Richtmyer, D., and K.W. Morton [1967], *Difference Methods for Initial Value Problems*, Second edition, Interscience, New York.

Simo, J.C. [1985], "A finite strain beam formulation. The three dimensional dynamic problem. Part I," *Comp. Meth. Appl. Mech. Engrg.*, Vol. 49, pp. 55-70.

Simo, J.C., and L. Vu Quoc [1985], "Three dimensional finite strain rod model. Part II: Computational aspects," *Electronics Research Laboratory Memorandum No. UCB/ERL M85/31*, University of California, Berkeley (submmitted for publication in *Comp. Meth. Appl. Mech. Engrg.*).

Song, J.O., and E.J. Haug [1980], "Dynamic analysis of planar flexible mechanism," *Comp. Meth. Appl. Mech. Engrg.*, Vol. 24, pp. 359-381.

Sunada W., and S. Dubowsky [1980], "The application of finite element method to the dynamic analysis of flexible spatial and co-planar linkage systems," *J. of Mechanical Design*, Vol. 103, pp. 643-651.

Winfrey, R.C. [1971], "Elastic link mechanism dynamics," *Trans. ASME, J. of Engineering for Industry*, Vol. 93, No. 1, pp. 268-272.

Zienkiewicz, O.C. [1977], *The Finite Element Method*, third edition, Mc Graw-Hill, New York.

Appendix: Finite element matrices.

In this appendix, we shall give the expressions of the relevant matrices discussed in section 4; namely, the mass matrix $\mathbf{M}$, the internal forces vector $\mathbf{P}(\mathbf{d})$, the tangent stiffness matrix $\mathbf{K}_T(\mathbf{d})$, and the applied forces vector $\mathbf{F}(t)$.

Using the spatial discretization (4.3) in the first term of the weak form of the equations of motion (4.2), i.e., the inertia term, the mass matrix is obtained at once as

$$\boxed{\mathbf{M} = \int_{[0,L]} \Psi^t(X_1)\, \mathrm{I}\, \Psi(X_1)\, dX_1} \tag{A.1a}$$

with

$$\Psi(X_1) := [\Psi_1(X_1),....,\Psi_N(X_1)] \tag{A.1b}$$

Next, by making use of (3.14) and (3.15), we may rephrase the second term in the weak form (4.2) as follows

$$\boldsymbol{\eta} := \eta_1 \mathbf{e}_1 + \eta_2 \mathbf{e}_2 + \eta_3 \mathbf{e}_3 ,$$

$$\int_{[0,L]} \boldsymbol{\eta} \cdot \mathbb{P}[\mathbf{d}]\, dX_1 = - \int_{[0,L]} [\eta_1 n_1' + \eta_2 n_2' + \eta_3 m' + \eta_3\{(1+u_1')n_2 - u_2' n_1\}]\, dX_1 \tag{A.2}$$

Integrate by parts $(A.2)_2$, and recall that $\boldsymbol{\eta} \cdot [n_1, n_2, m]^t \Big|_{X_1=0}^{X_1=L} \equiv 0$; there results

$$\int_{[0,L]} \boldsymbol{\eta} \cdot \mathbb{P}[\mathbf{d}]\, dX_1 = \int_{[0,L]} \mathbf{D}_1(\mathbf{d})\, \boldsymbol{\eta} \cdot \begin{Bmatrix} n_1(\mathbf{d}) \\ n_2(\mathbf{d}) \\ m(\mathbf{d}) \end{Bmatrix} dX_1 \tag{A.3a}$$

with $\mathbf{D}_1(\mathbf{d})$ denoting the following differential operator

$$\mathbf{D}_1(\mathbf{d}) := \begin{bmatrix} d/dX_1 & 0 & u_2' \\ 0 & d/dX_1 & -(1+u_1') \\ 0 & 0 & d/dX_1 \end{bmatrix} \tag{A.3b}$$

Introducing the discretization $(4.3)_2$ into (A.3a), we obtain the expression for the discrete internal forces

$$\boxed{\mathbf{P}(\mathbf{d}^h) = \int_{[0,L]} [\mathbf{D}_1(\mathbf{d}^h)\Psi(X_1)]^t \begin{Bmatrix} n_1(\mathbf{d}^h) \\ n_2(\mathbf{d}^h) \\ m(\mathbf{d}^h) \end{Bmatrix} dX_1} \tag{A.4}$$

In (A.4), the superscript h in $\mathbf{d}^h$ is used to designate the spatial approximation to $\mathbf{d}(X_1, t)$ according to $(4.3)_1$. The same notation will be used throughout in this appendix.

We now undertake the linearization of $\int_{[0,L]} \boldsymbol{\eta}\cdot\mathbb{P}[\mathbf{d}]dX_1$ about a fixed configuration $\mathbf{d} \equiv \hat{\mathbf{d}}$. This linearization procedure and the spatial discretization (4.3), leads to the expression for the tangent stiffness matrix $\mathbf{K}_T(\hat{\mathbf{d}})$ appearing in (4.9). For the developments that follow, it proves convenient to rewrite (3.15) as

$$\begin{Bmatrix} N_1(\mathbf{d}) \\ N_2(\mathbf{d}) \\ M(\mathbf{d}) \end{Bmatrix} := \hat{\mathbf{C}} \left[\hat{\mathbf{\Lambda}}^t(\mathbf{d}) \begin{Bmatrix} 1+u_1' \\ u_2' \\ \vartheta' \end{Bmatrix} - \begin{Bmatrix} 1 \\ 0 \\ 0 \end{Bmatrix} \right], \quad \begin{Bmatrix} n_1(\mathbf{d}) \\ n_2(\mathbf{d}) \\ m(\mathbf{q}) \end{Bmatrix} = \hat{\mathbf{\Lambda}}(\mathbf{d}) \begin{Bmatrix} N_1(\mathbf{d}) \\ N_2(\mathbf{d}) \\ M(\mathbf{d}) \end{Bmatrix} \tag{A.5a}$$

where

$$\hat{\mathbf{C}} := Diag[EA, GA_s, EI], \quad \hat{\mathbf{\Lambda}}(\mathbf{d}) := \begin{bmatrix} \cos\vartheta & -\sin\vartheta & 0 \\ \sin\vartheta & \cos\vartheta & 0 \\ 0 & 0 & 1 \end{bmatrix} \tag{A.5b}$$

The linearization about $\hat{\mathbf{d}}$ is based on the notion of directional derivative at $\hat{\mathbf{d}}$ in the direction $\Delta\mathbf{d} := [\Delta u_1, \Delta u_2, \Delta\vartheta]^t$. The following linearized quantities are needed:

$$\frac{d}{d\varepsilon}\bigg|_{\varepsilon=0} \hat{\mathbf{\Lambda}}(\hat{\mathbf{d}} + \varepsilon\Delta\mathbf{d}) = \begin{bmatrix} 0 & -\Delta\vartheta & 0 \\ \Delta\vartheta & 0 & 0 \\ 0 & 0 & 0 \end{bmatrix} \hat{\mathbf{\Lambda}}(\hat{\mathbf{d}}), \tag{A.6a}$$

$$\frac{d}{d\varepsilon}\bigg|_{\varepsilon=0} \begin{Bmatrix} N_1 \\ N_2 \\ M \end{Bmatrix} (\hat{\mathbf{d}} + \varepsilon\Delta\mathbf{d}) = \hat{\mathbf{C}}\hat{\mathbf{\Lambda}}(\hat{\mathbf{d}})\mathbf{D}_1(\hat{\mathbf{d}})\Delta\mathbf{d}, \tag{A.6b}$$

$$\frac{d}{d\varepsilon}\bigg|_{\varepsilon=0} \mathbf{D}_1(\hat{\mathbf{d}} + \varepsilon\Delta\mathbf{d})\boldsymbol{\eta} = \begin{bmatrix} 0 & 0 & \Delta u_2' \\ 0 & 0 & -\Delta u_1' \\ 0 & 0 & 0 \end{bmatrix} \boldsymbol{\eta}. \tag{A.6c}$$

The linearization of the second term in the weak form (4.2) then follows at once

$$\boxed{\begin{aligned}&\frac{d}{d\varepsilon}\Big|_{\varepsilon=0}\ \{\int_{[0,L]}\boldsymbol{\eta}\cdot\mathbb{P}[\hat{\mathbf{d}}+\varepsilon\Delta\mathbf{d}]\ dX_1\}\ =\\&\int_{[0,L]}\mathbf{D}_1(\hat{\mathbf{d}})\boldsymbol{\eta}\cdot\hat{\boldsymbol{\Lambda}}(\hat{\mathbf{d}})\,\hat{\mathbf{C}}\,\hat{\boldsymbol{\Lambda}}^t(\hat{\mathbf{d}})\,\mathbf{D}_1(\hat{\mathbf{d}})\,\Delta\mathbf{d}\ dX_1\\&+\int_{[0,L]}\mathbf{D}_2\boldsymbol{\eta}\cdot\mathbf{G}(\hat{\mathbf{d}})\,\mathbf{D}_2\Delta\mathbf{d}\ dX_1\end{aligned}}\qquad(A.7)$$

in which the differential operator $\mathbf{D}_2$ and the matrix $\mathbf{G}(\hat{\mathbf{d}})$ are defined below

$$\mathbf{D}_2 := Diag[\,d/dX_1,\ d/dX_1,\ 1\,],$$
$$\mathbf{G}(\hat{\mathbf{d}}) := \begin{bmatrix}0 & 0 & -n_2(\hat{\mathbf{d}})\\ 0 & 0 & n_1(\hat{\mathbf{d}})\\ -n_2(\hat{\mathbf{d}}) & n_1(\hat{\mathbf{d}}) & -[(1+\hat{u}_1')n_1(\hat{\mathbf{d}})+\hat{u}_2'n_2(\hat{\mathbf{d}})]\end{bmatrix}\qquad(A.8)$$

Let us now introduce the spatial discretization of $\Delta\mathbf{d}(X_1)$ in the same manner as in $(4.3)_1$

$$\Delta\mathbf{d}(X_1)\ \cong\ \sum_{I=1}^{N}\Psi(X_1)\,\Delta\mathbf{q}_I\qquad(A.9)$$

Using (4.3) together with (A.9), we finally arrive at the expression for the tangent stiffness matrix at $\hat{\mathbf{d}}^h \cong \hat{\mathbf{d}}$

$$\boxed{\mathbf{K}_T(\hat{\mathbf{d}}^h)\ =\ \mathbf{K}(\hat{\mathbf{d}}^h)+\mathbf{K}_G(\hat{\mathbf{d}}^h)}\qquad(A.10)$$

where $\mathbf{K}(\hat{\mathbf{d}}^h)$ represents the *material* part of the tangent stiffness,

$$\boxed{\mathbf{K}(\hat{\mathbf{d}}^h)\ :=\ \int_{[0,L]}[\mathbf{D}_1(\hat{\mathbf{d}}^h)\Psi(X_1)]^t\,\hat{\boldsymbol{\Lambda}}(\hat{\mathbf{d}}^h)\,\hat{\mathbf{C}}\,\hat{\boldsymbol{\Lambda}}^t(\hat{\mathbf{d}}^h)\,\mathbf{D}_1(\hat{\mathbf{d}}^h)\,\Psi(X_1)\ dX_1}\qquad(A.11)$$

and $\mathbf{K}_G(\hat{\mathbf{d}}^h)$ the *geometric* part,

$$\boxed{\mathbf{K}_G(\hat{\mathbf{d}}^h)\ :=\ \int_{[0,L]}[\mathbf{D}_2\Psi(X_1)]^t\,\mathbf{G}(\hat{\mathbf{d}}^h)\,\mathbf{D}_2\Psi(X_1)\ dX_1}\qquad(A.12)$$

It is clear that the applied load vector $\mathbf{F}(t)$ is given by

$$\boxed{\mathbf{F}(t)\ =\ \int_{[0,L]}\Psi^t(X_1)\begin{Bmatrix}\bar{n}_1(X_1,t)\\ \bar{n}_2(X_1,t)\\ \bar{m}(X_1,t)\end{Bmatrix}dX_1}\qquad(A.13)$$

The integration in all of the above matrices may be performed numerically using Gauss quadrature. For the tangent stiffness matrix $\mathbf{K}_T$, we use uniform reduced integration to avoid shear locking. •

Figure Captions.

Figure 2.1. *Basic kinematics.* Floating and inertial frames.

Figure 3.1. Physical interpretation of the strain components of a beam in the finite strain case.

Figure 5.1.1.a. *Displacement driven flexible robot arm.* Problem data.

Figure 5.1.1.b. *Displacement driven flexible robot arm.* Repositioning sequence to stop angle $\psi = 1.5\ rad$. Time step size $h = 0.5$.

Figure 5.1.1.c. *Displacement driven flexible robot arm.* Free vibration about $\psi = 1.5\ rad$. Time step size $h = 0.5$.

Figure 5.1.2.a. *Force driven flexible robot arm.* Problem data.

Figure 5.1.2.b. *Force driven flexible robot arm.* Sequence of motion during application of torque. Time step size $h = 0.5$.

Figure 5.1.2.c. *Force driven flexible robot arm.* Sequence of motion after removal of applied torque — completion of one revolution. Time step size $h = 0.5$.

Figure 5.2.1.a. *Flexible beam in free flight.* Problem data.

Figure 5.2.1.b. *Flexible beam in free flight.* Sequence of motions during application of loading. Time step size $h = 0.1$, plot after each 5 time increments.

Figure 5.2.1.c. *Flexible beam in free flight.* Free flight of the beam after removal of the loading — close-up on the first 2 revolutions. Time step size $h = 0.1$, plot after each 5 time increments.

Figure 5.2.1.d. *Flexible beam in free flight.* Free flight —entire sequence.

Figure 5.2.2. *The "flying spaghetti."* Time step size $h = 0.1$, plot after each 5 time increments.

Figure 5.3.1.a. *Multibody dynamics*: Displacement driven of multi-component robot arm. Problem data.

Figure 5.3.1.b. *Multibody dynamics*: Displacement driven of multi-component robot arm. Repositioning sequence to stop angle $\psi = 1.5 rad$. Time step size $h = 0.1$.

Figure 5.3.1.c. *Multibody dynamics*: Displacement driven of multi-component robot arm. Vibration of robot arm about stop angle, and revolution of flexible appendage about connecting hinge. Time step size $h = 0.01$, plot after each 10 time increments.

Figure 5.3.2. *Multibody dynamics*: Articulated beam in free flight. Time step size $h = 0.05$, plot after each 5 time increments.

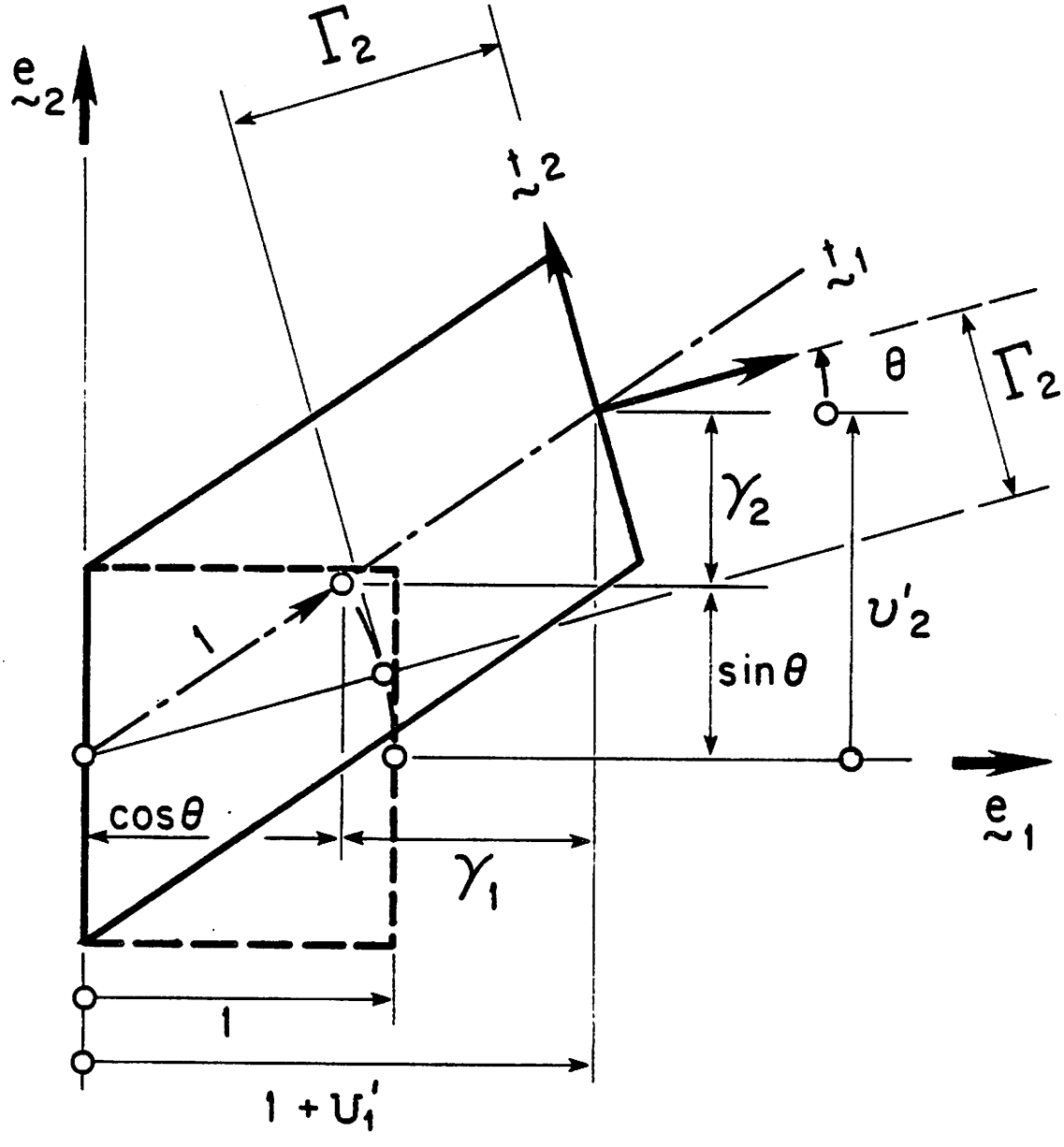

Figure 2.1. *Basic kinematics.* Floating and inertial frames.

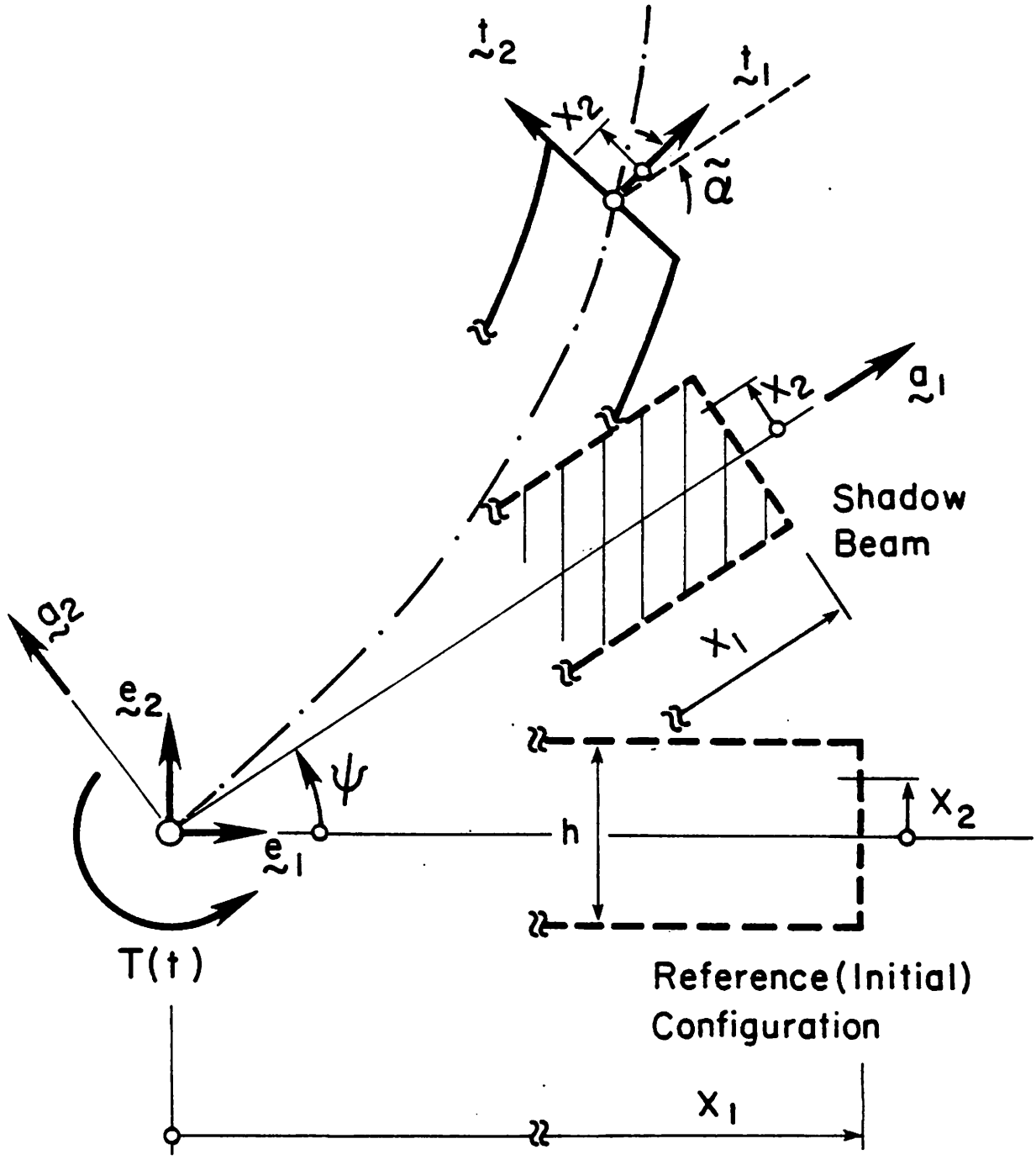

Figure 3.1. Physical interpretation of the strain components of a beam in the finite strain case.

Material Properties:

$EA = GA_s = 10{,}000.$

$EI = 1{,}000.$

$A_\rho = 1.$

$I_\rho = 10.$

F.e. Mesh: 10 linear elements

Time history of $\psi(t)$:

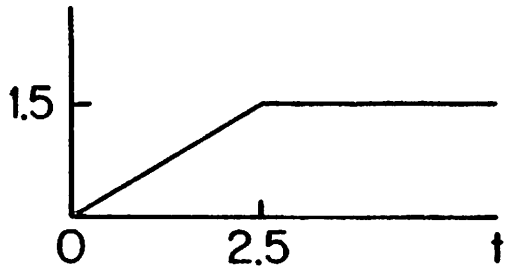

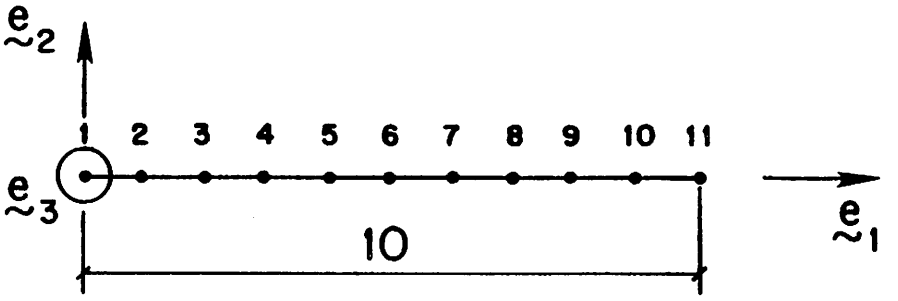

Figure 5.1.1.a. *Displacement driven flexible robot arm.* Problem data.

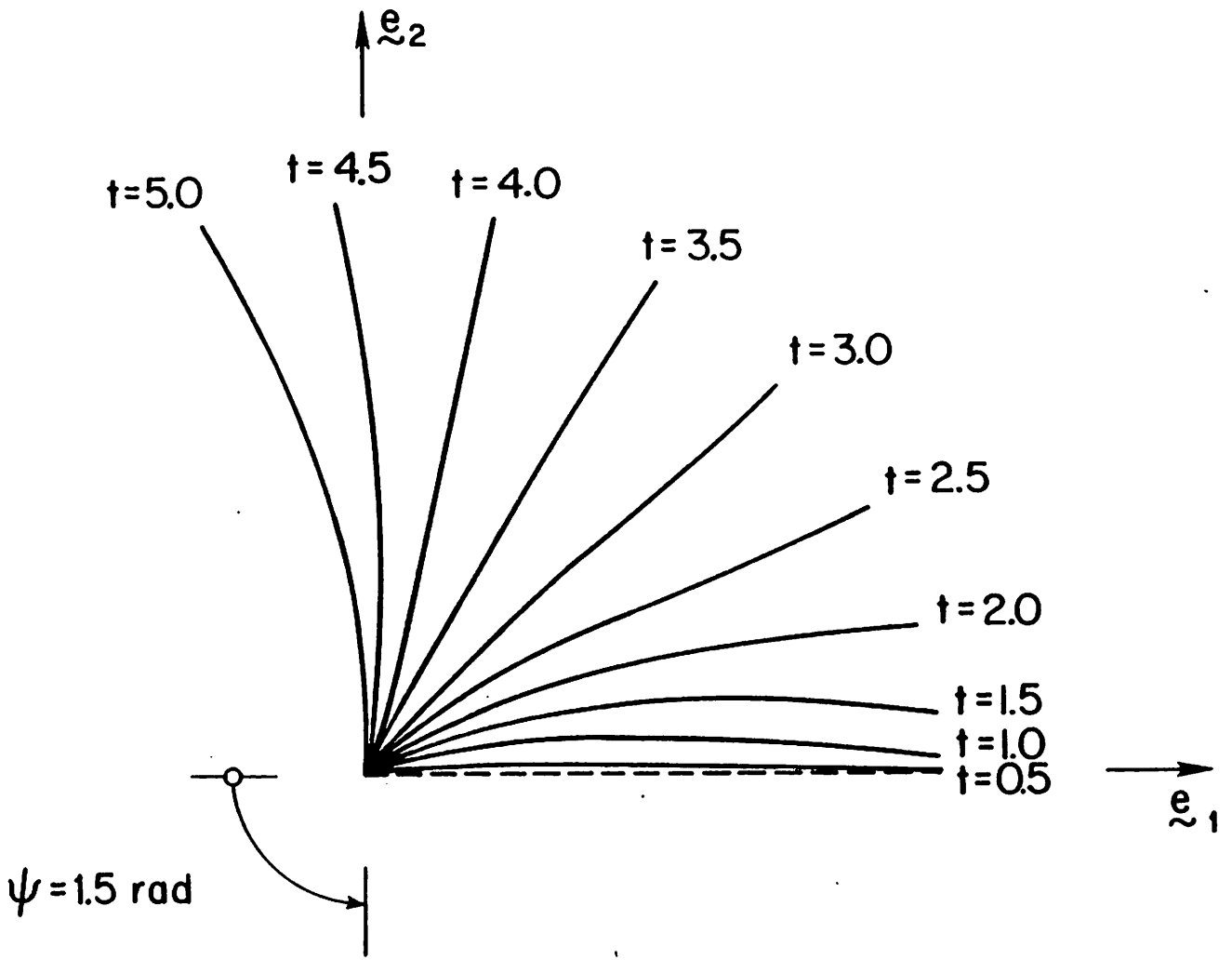

Figure 5.1.1.b. *Displacement driven flexible robot arm.* Repositioning sequence to stop angle $\psi = 1.5$ *rad*. Time step size $h = 0.5$.

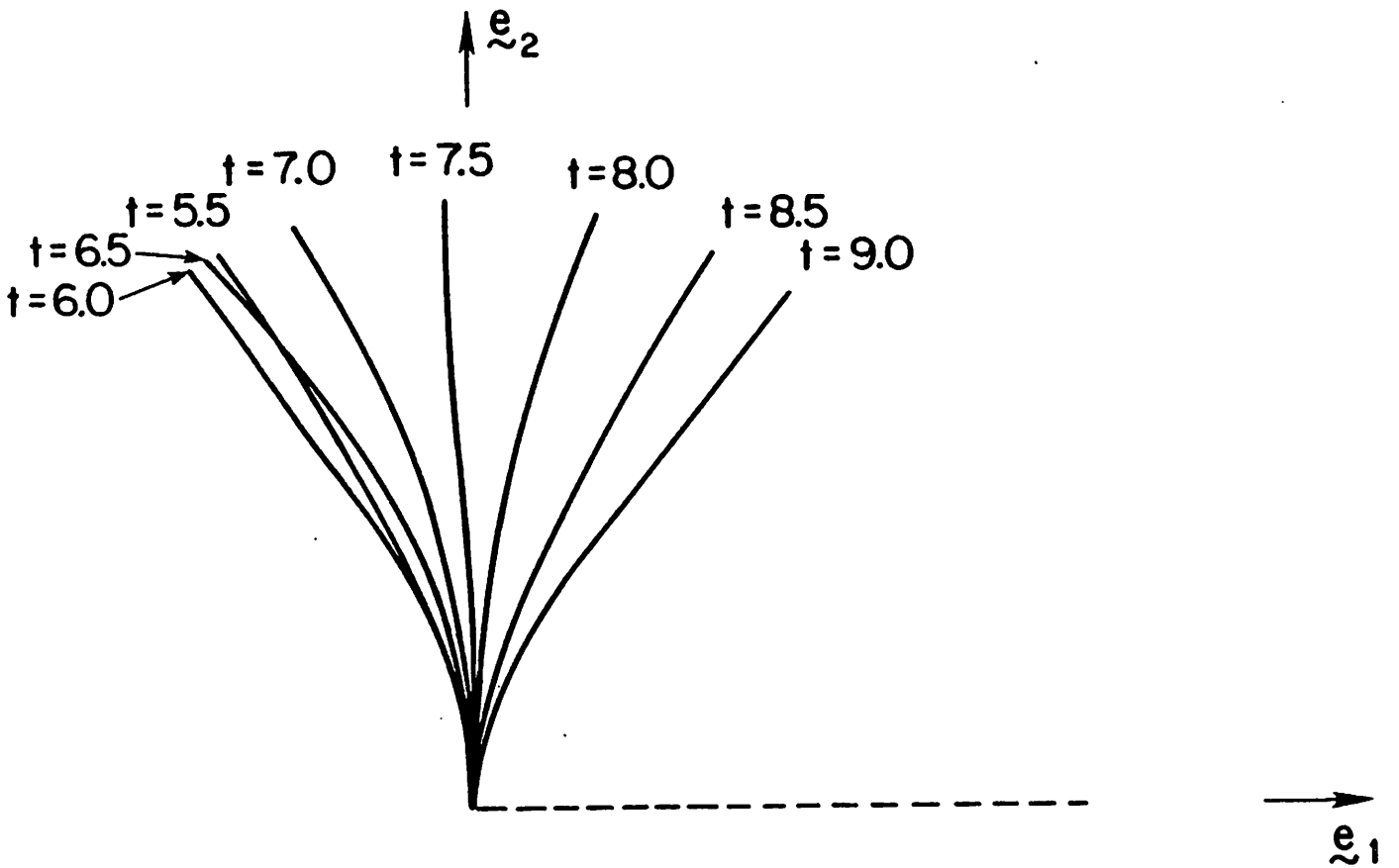

Figure 5.1.1.c. *Displacement driven flexible robot arm.* Free vibration about $\psi = 1.5$ *rad*. Time step size $h = 0.5$.

Material Properties:

$EA = GA_s = 10{,}000.$

$EI = 1{,}000.$

$A_\rho = 1.$

$I_\rho = 10.$

F.e. Mesh: 10 linear elements.

Time history of T(t):

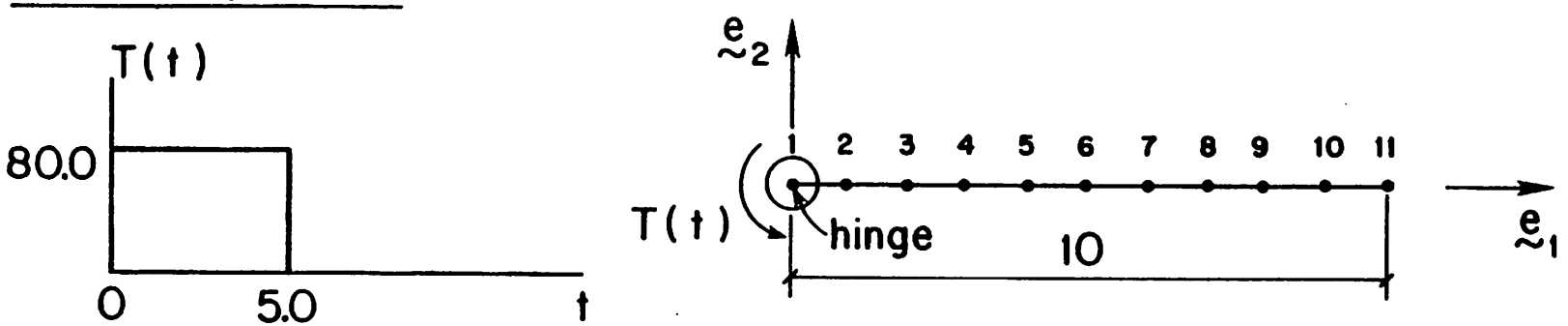

Figure 5.1.2.a. *Force driven flexible robot arm.* Problem data.

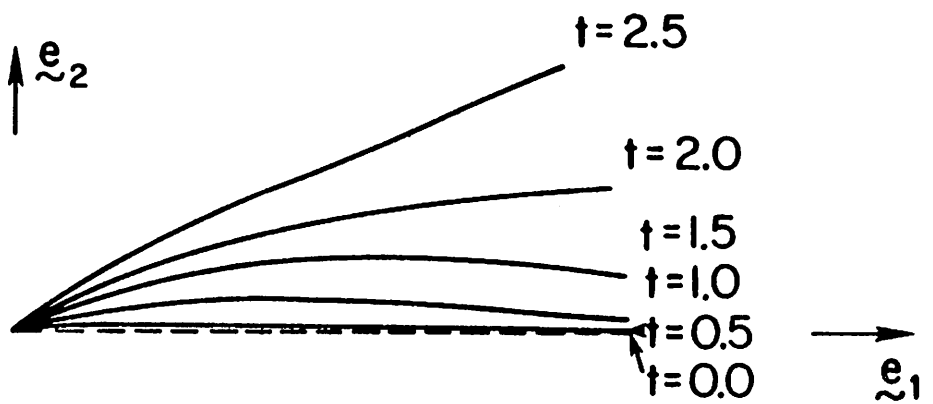

Figure 5.1.2.b. *Force driven flexible robot arm.* Sequence of motion during application of torque. Time step size $h = 0.5$.

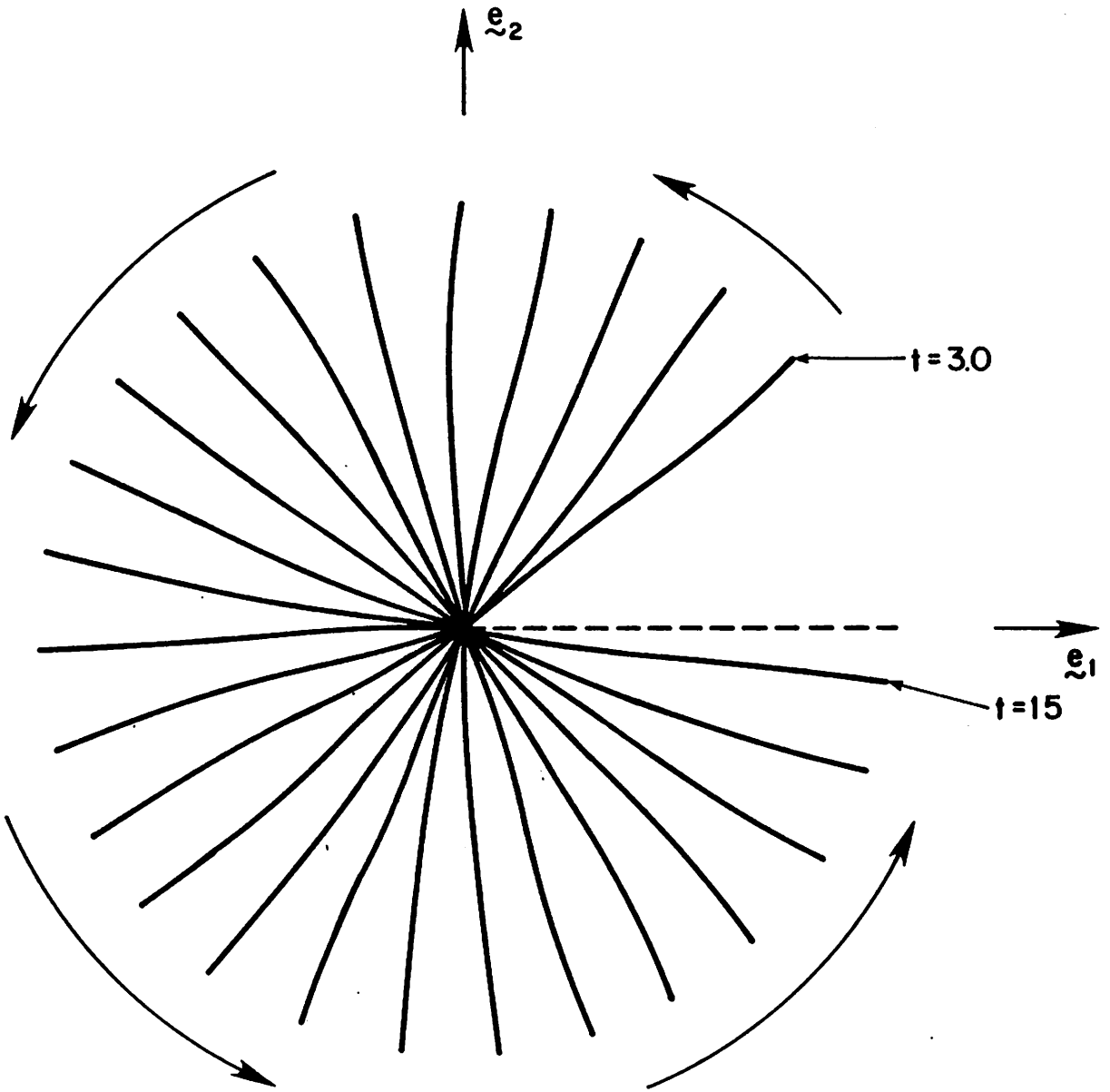

Figure 5.1.2.c. *Force driven flexible robot arm.* Sequence of motion after removal of applied torque — completion of one revolution. Time step size $h = 0.5$.

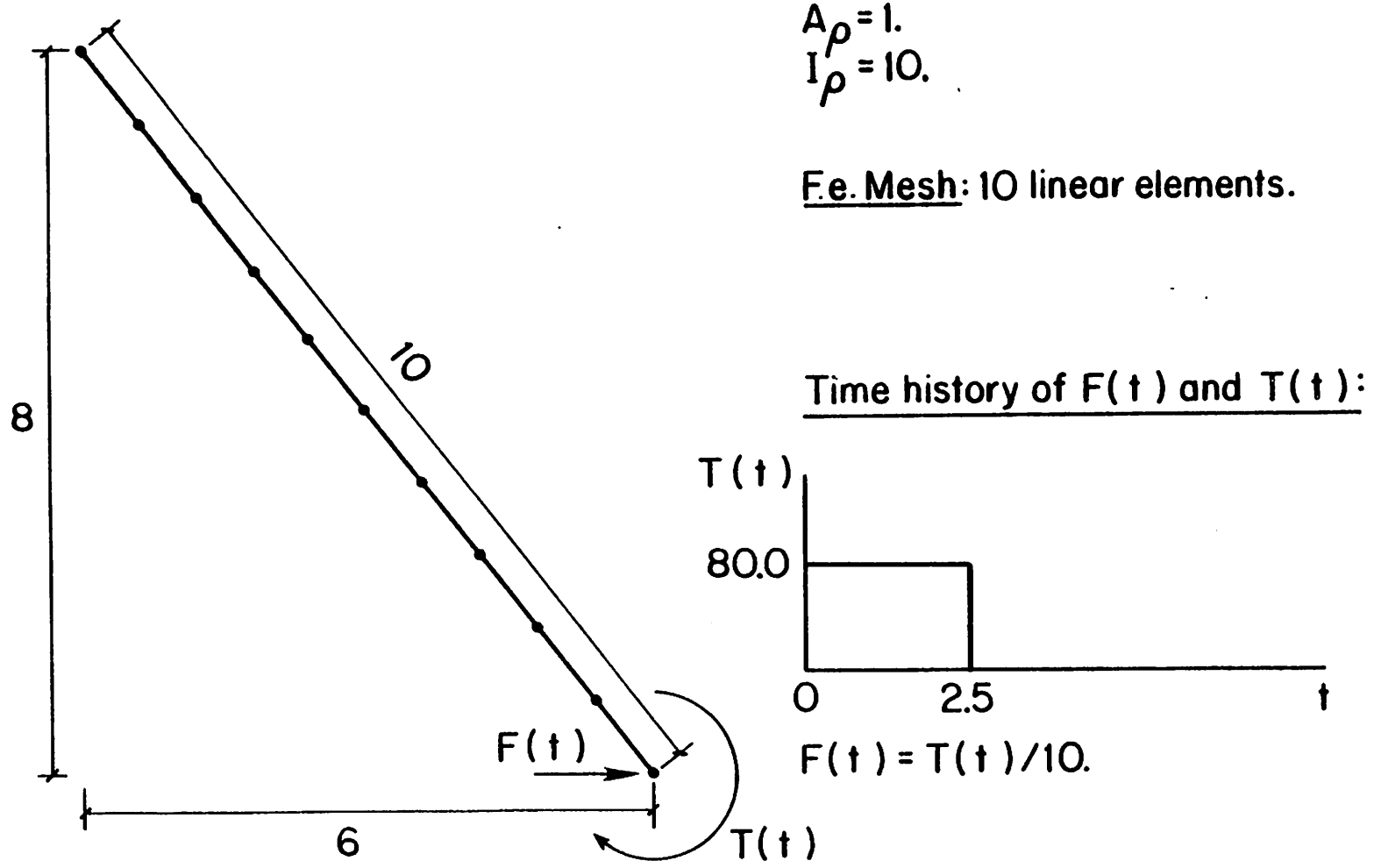

Figure 5.2.1.a. *Flexible beam in free flight.* Problem data.

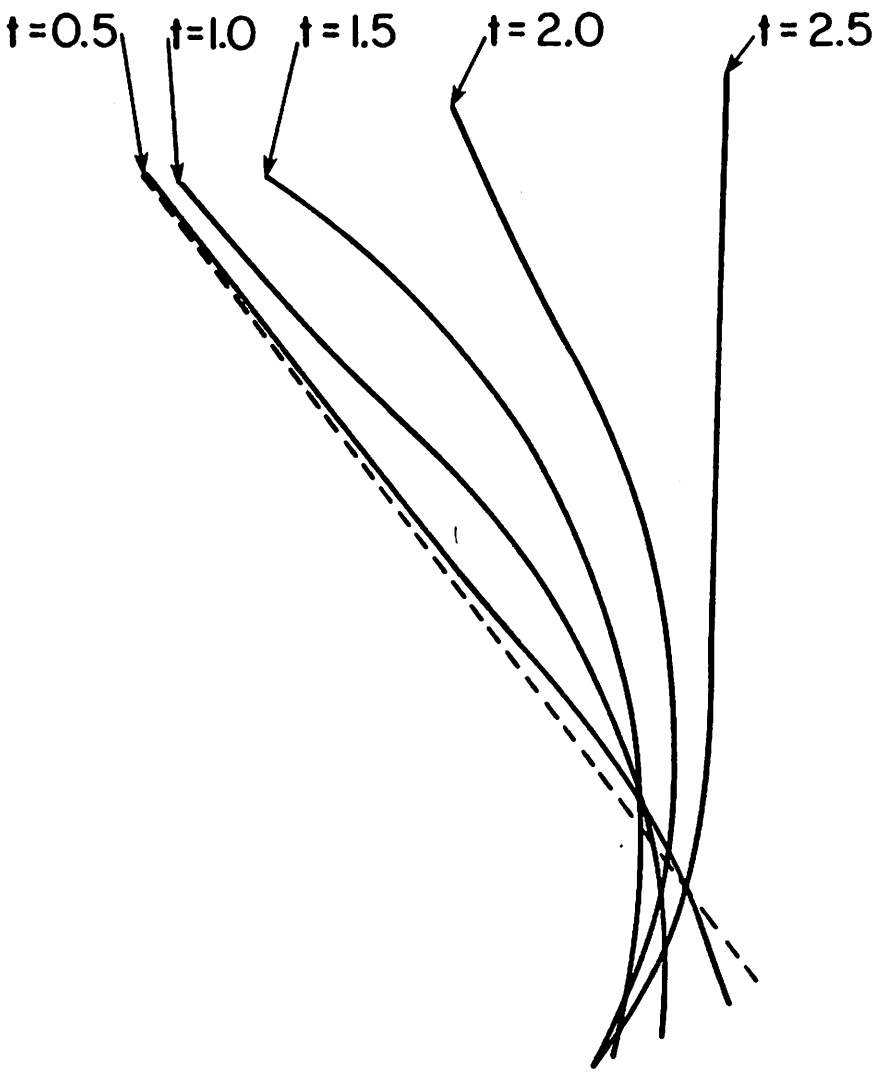

Figure 5.2.1.b. *Flexible beam in free flight.* Sequence of motions during application of loading. Time step size $h = 0.1$, plot after each 5 time increments.

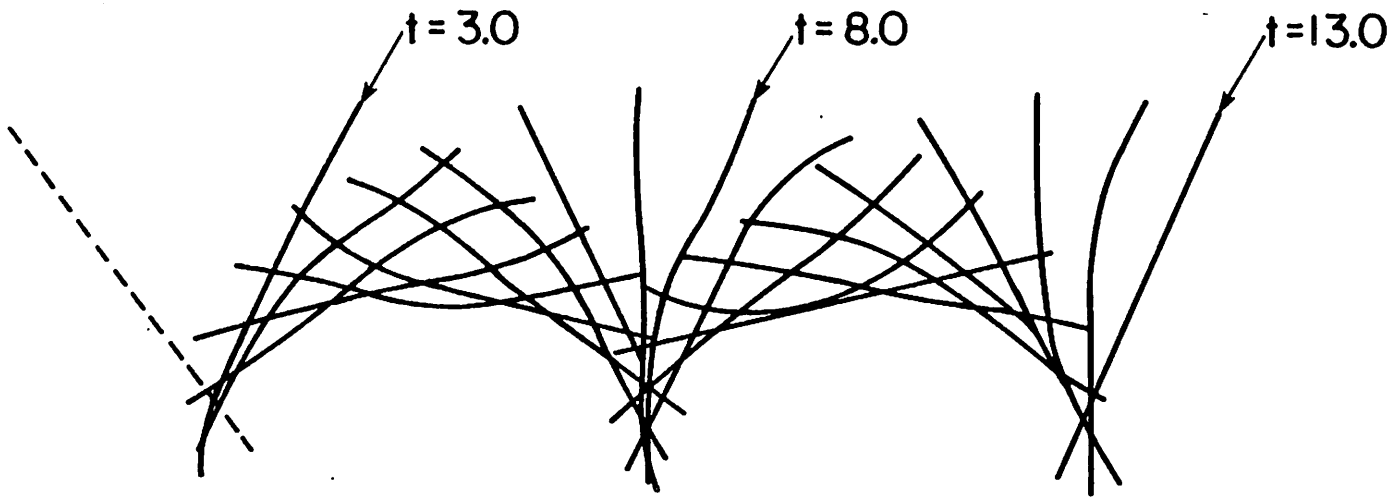

Figure 5.2.1.c. *Flexible beam in free flight.* Free flight of the beam after removal of the loading — close-up on the first 2 revolutions. Time step size $h = 0.1$, plot after each 5 time increments.

Figure 5.2.1.d. *Flexible beam in free flight.* Free flight — entire sequence.

Material Properties:

$EA = GA_s = 10{,}000.$

$EI = 100.$

$A_\rho = 1.$

$I_\rho = 10.$

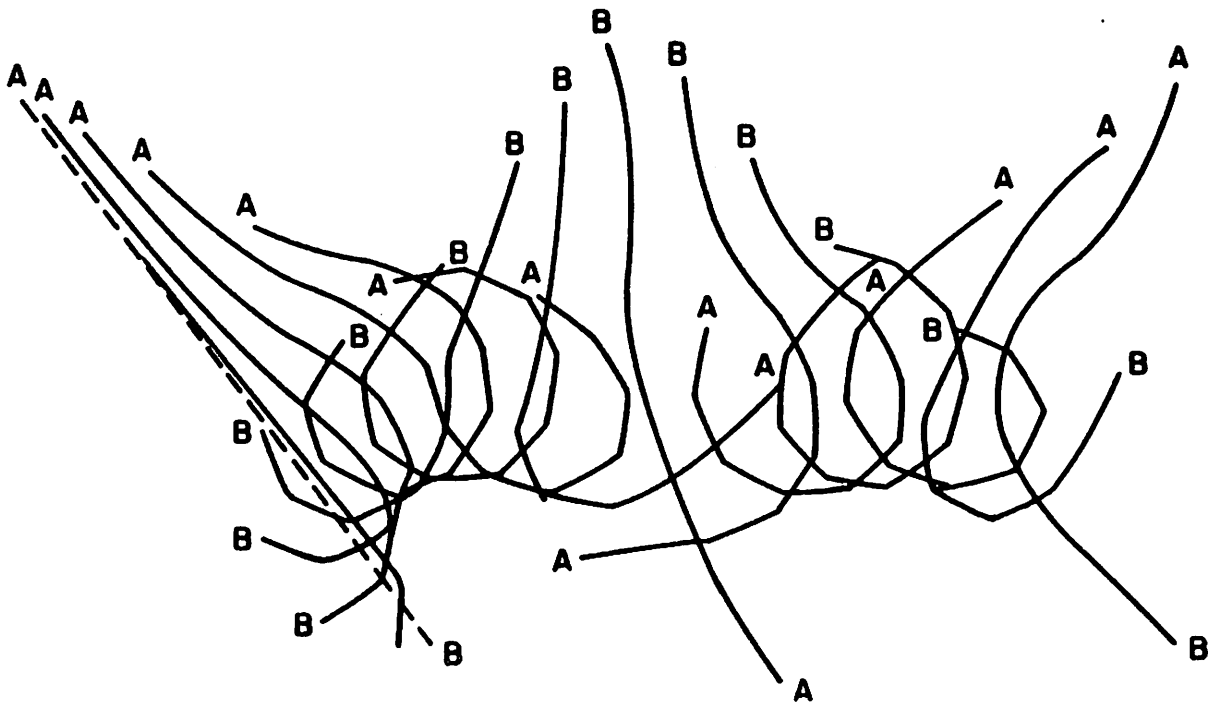

Figure 5.2.2. *The "flying spaghetti."* Time step size $h = 0.1$, plot after each 5 time increments.

Material Properties:

$EA = GA_s = 1{,}000{,}000.$

$EI = 100{,}000.$

$A_\rho = 1.$

$I_\rho = 1.$

F.e. Mesh: 4 quadratic elements.

Time history of $\psi(t)$:

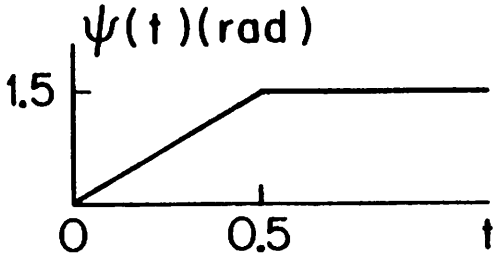

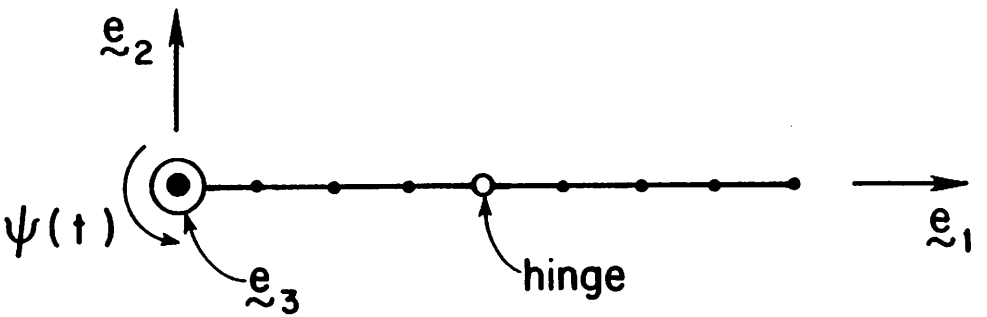

Figure 5.3.1.a. *Multibody dynamics*: Displacement driven of multi-component robot arm. Problem data.

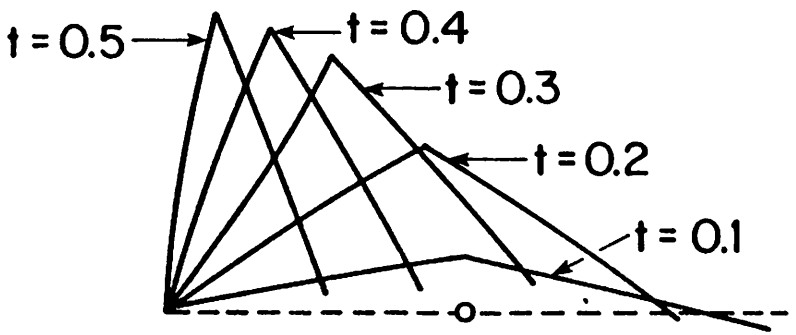

Figure 5.3.1.b. *Multibody dynamics*: Displacement driven of multi-component robot arm. Repositioning sequence to stop angle $\psi = 1.5rad$. Time step size $h = 0.1$.

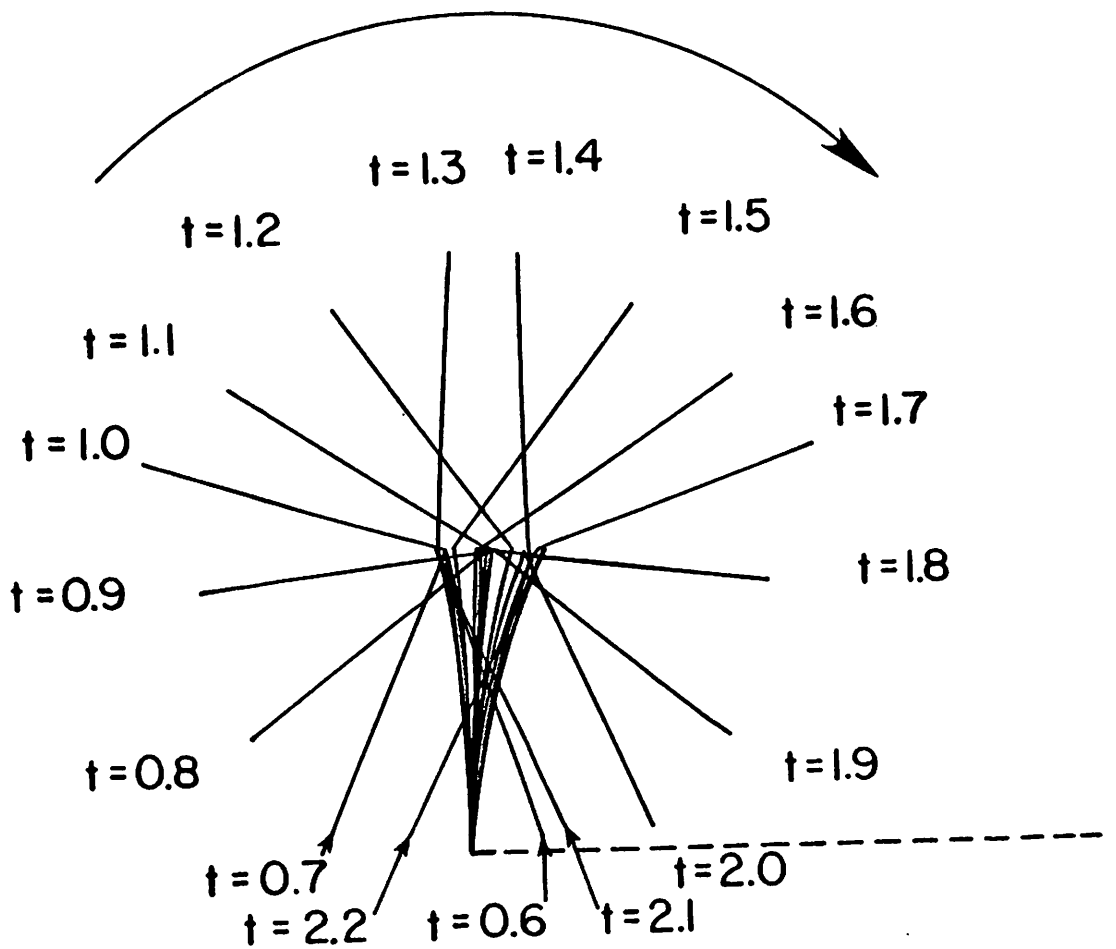

Figure 5.3.1.c. *Multibody dynamics*: Displacement driven of multi-component robot arm. Vibration of robot arm about stop angle, and revolution of flexible appendage about connecting hinge. Time step size $h = 0.01$, plot after each 10 time increments.

Material Properties:

$EA = GA_s = 1{,}000{,}000.$

$EI = 10{,}000.$

$A\rho = 1.$

$I\rho = 1.$ for link A

$I\rho = 10.$ for link B

F.e. Mesh: 4 quadratic elements.

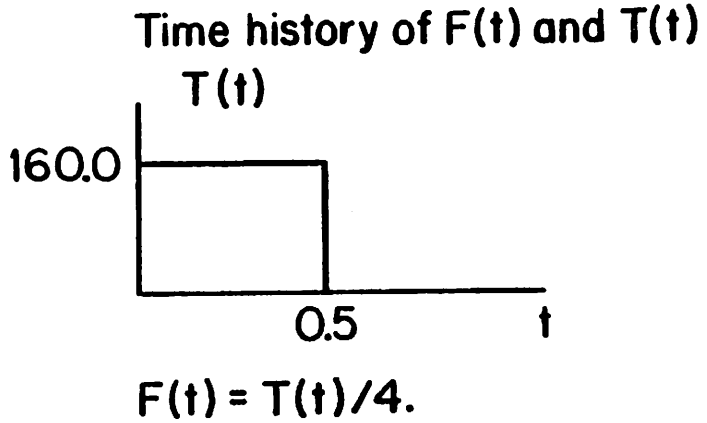

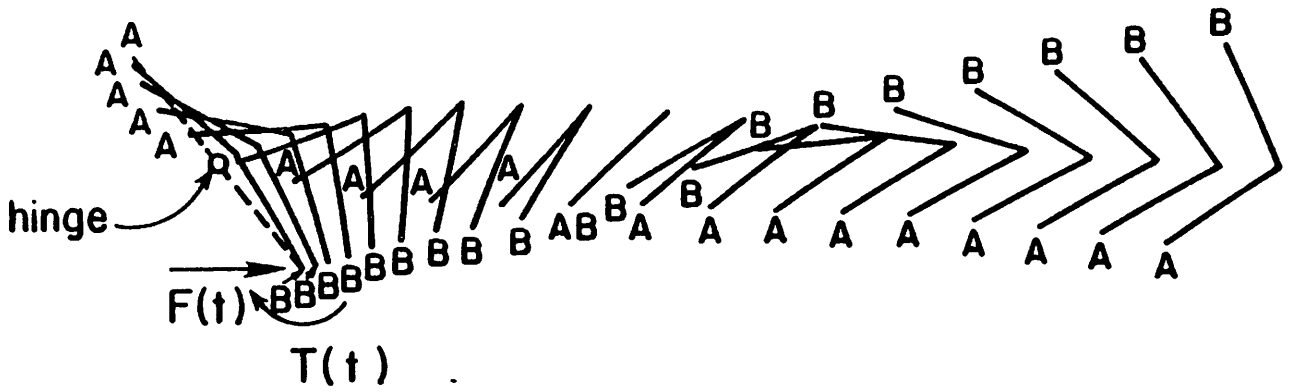

Figure 5.3.2. *Multibody dynamics*: Articulated beam in free flight. Time step size $h = 0.05$, plot after each 5 time increments.